BRNO UNIVERSITY OF TECHNOLOGY

Faculty of Chemistry

MASTER'S THESIS

Brno, 2020 Bc. Anna Koukolová

BRNO UNIVERSITY OF TECHNOLOGY
VYSOKÉ UČENÍ TECHNICKÉ V BRNĚ

FACULTY OF CHEMISTRY
FAKULTA CHEMICKÁ

INSTITUTE OF PHYSICAL AND APPLIED CHEMISTRY
ÚSTAV FYZIKÁLNÍ A SPOTŘEBNÍ CHEMIE

STUDIES TOWARDS THE PREPARATION OF ORGANIC-INORGANIC HYBRID SILICA FIBERS VIA ELECTROSPINNING

STUDIUM PŘÍPRAVY HYBRIDNÍCH ORGANOKŘEMIČITÝCH POLYMERNÍCH VLÁKEN METODOU ELEKTROSTATICKÉHO ZVLÁKŇOVÁNÍ

MASTER'S THESIS
DIPLOMOVÁ PRÁCE

AUTHOR
AUTOR PRÁCE

Bc. Anna Koukolová

SUPERVISOR
VEDOUCÍ PRÁCE

Prof. Dr. Nicola Hüsing

BRNO 2020

BRNO UNIVERSITY OF TECHNOLOGY
FACULTY OF CHEMISTRY

Specification Master's Thesis

Project no.:	FCH-DIP1472/2019	Academic year:	2019/20
Department:	Institute of Physical and Applied Chemistry		
Student:	**Bc. Anna Koukolová**		
Study programme:	Consumer Chemistry		
Study branch:	Consumer Chemistry		
Head of thesis:	**Prof. Dr. Nicola Hüsing**		

Title of Master's Thesis:

Studies towards the Preparation of Organic–Inorganic Hybrid Silica Fibers via Electrospinning

Master's Thesis:

1. The goal of the master thesis is the successful synthesis of polyvinylsiloxane nanofibers by using a sol–gel derived electrospinning method.
2. The project will start with an extensive literature research on the state of the art of the electrospinning of siloxanes and other sol–gel derived materials.
3. The student will get familiar with the electrospinning process and its possibility of producing polysiloxane based electrospun fibrous materials. The task will be to evaluate the parameters of the electrospinning process in terms of polyvinylsiloxanes and the electrospinning procedure itself.
4. Resulting fibrous materials will be characterized with different techniques in order to compare them with conventional nano–scale materials and to investigate application possibilities.

Deadline for Master's Thesis delivery: 31.7.2020:

Master's Thesis should be submitted to the institute's secretariat in a number of copies as set by the dean This specification is part of Master's Thesis

Bc. Anna Koukolová Student	Prof. Dr. Nicola Hüsing Head of thesis	prof. Ing. Miloslav Pekař, CSc. Head of department

In Brno dated 31.1.2020

prof. Ing. Martin Weiter, Ph.D.
Dean

ABSTRACT

Polyorganosilanes are an emerging class II hybrid material potentially enabling the preparation of new materials with novel functionalities. Although some pertinent intriguing materials and applications have been investigated, to date, the preparation of polyorganosilane-based micro and nanofibers has not been reported. Therefore, the present thesis deals with the investigation of poly(vinylmethyldimethoxysilane) as a novel precursor for the preparation of fibers via electrospinning.

Free-radical bulk polymerization of vinylmethyldimethoxysilane was performed in order to obtain polymeric products of various molecular weights. The degree of polymerization was studied with respect to the radical starter concentration by dynamic light scattering and nuclear magnetic resonance spectroscopy experiments. Investigations of the ability to form fibers by electrospinning from solutions of the synthetized polymers were conducted with special emphasis on the properties of the used polymeric product and the spinning solution.

Results showed that the studied polymer is in principle suitable for the preparation of fibers. However, only fragments of fibers were obtained by electrospinning of the polymers using methanol as a solvent. Further investigations, employing a sol-gel processing approach in order to enhance the number of polymer chain entanglements and thus increase spinnability, were conducted. It was found that the stage of gelation was crucial and the sol-gel process was investigated towards several parameters such as gelation time with respect to pH and water content. Again, fiber fragments could be obtained using optimized sol-gel processing parameters. Finally, a strategy utilizing a carrier polymer successfully yielded polyorganosilane-based fibers and the resulting fiber morphology was correlated to the employed process parameters.

KEYWORDS

Electrospinning, fibers, polyvinylsiloxane, free-radical polymerization, sol-gel processing.

ABSTRAKT

Polyorganosilany spadají do skupiny hybridních materiálů třídy II, které nabízejí nové možnosti materiálových funkcí a jejich vlastností. Ačkoliv byly v této kategorii již některé materiály zkoumány a stejně tak i jejich aplikace, nebyly doposud vlákna na základě polyorganosilanu v mikro a nano rozměru popsány což bylo motivací pro tuto práci. Předkládaná diplomová práce se zabývá podrobným zkoumáním poly(vinylmethyldimethoxysilanu) jako možného prekurzoru pro elektrostatické zvlákňování.

Za účelem přípravy polymeru na bázi vinylmethylsilanu byla provedena radikálová polymerace a podmínky reakce byly modifikovány se záměrem změny molekulové hmotnosti získaného polymeru. Stupeň polymerace byl upravován na základě změny koncentrace iniciátoru a byl stanovován dynamickým rozptylem světla v roztoku polymeru a spektroskopickou metodou nukleární magnetické rezonance. Elektrostatické zvlákňování je velkou měrou spojeno s vlastnostmi roztoku a důraz byl proto kladen právě na zjištění těchto vlastností.

Na základě experimentů bylo zjištěno, že syntetizovaný polymer je na přípravu vláken vhodný. Nicméně byly získány i fragmenty vláken a to s využitím polymeru v roztoku methanolu. Předpokladem zvlákňování je dostatek propojení mezi polymerními řetězci. Tento přístup byl studován se zapojením sol-gel postupu a bylo zjištěno, že fáze sol-gel procesu je velmi významná s ohledem na tvorbu vláken. Dalším využitým postupem pro získání vláken bylo začlenění dalšího polymeru do směsi jako nosiče a tímto postupem byla získána vlákna s různým průměrem.

KLÍČOVÁ SLOVA

Elektrostatické zvlákňování, vlákna, polyvinylsiloxan, radikálová polymerizace, sol-gel proces.

KOUKOLOVÁ, Anna. *Studies towards the Preparation of Organic-Inorganic Hybrid Silica Fibers via Electrospinning*. Brno, 2020. 79 p. Available on: https://www.vutbr.cz/studenti/zav-prace/detail/124060. Master thesis. Brno University of Technology, Faculty of Chemistry, Institute of Physical and Applied Chemistry. Supervised by Prof. Dr. Nicola Hüsing.

DECLARATION

I declare that the diploma thesis has been worked out by myself and that all the quotations from the used literary sources are accurate and complete. The content of the diploma thesis is the property of the Faculty of Chemistry of Brno University of Technology and all commercial uses are allowed only if approved by both the supervisor and the dean of the Faculty of Chemistry, BUT.

……..

Student's signature

ACKNOWLEDGEMENTS

Herein, I would like to express my gratitude to **Prof. Nicola Hüsing** as my thesis supervisor, mentor and facilitator as well. Thank you for giving me the opportunity to be a part of your lab at the University of Salzburg in the Materials Chemistry Group, as well as for your attitude and giving me a freedom in the project task.

Many thanks belong to **Daniel Euchler, MSc.** for his enthusiastic effort, giving me suggestions and advices throughout the project. From my humble beginning as a 4th-year student, Daniel has been extremely helpful and patient for which I cannot thank him enough. We have got along well together.

Dr. Christian Schuster is gratefully acknowledged for patient guidance and giving me encouragement. I must also express appreciation for discussions and text correction in a short period of time. Moreover, I am grateful for the assistance with NMR measurements.

I am indebted to **Hasan Razouq, MSc.** for introducing me electrospinning technique and device available at the department. **PD Dr. Raphael Berger** is acknowledged for the contribution to polymer simulations and IR results.

Furthermore, my gratitude belongs to all the other **colleagues from the 4th-floor** at the Department of Chemistry and Physics of Materials at the University of Salzburg for the kind working environment and giving of advices and help. Without the friendly atmosphere these people provided, this project would not have been as enjoyable as it was.

Prof. Miloslav Pekař from my alma mater Brno University of Technology is acknowledged for consultations and smooth workflow during the thesis project.

Last but not least, I would like to thank my **family, friends and supporters** for their constant encouragement and strong support, as well as being there through it all.

My motto and attitude for the project and stay in Austria was as follows: time and tide wait for no man. I had such a nice and fruitful time in Salzburg. And I would like to add a few Czech words to the end, adopted from **Jára Cimrman**: „Chválit se musíme sami. Tuhle práci za nás nikdo neudělá!“

My special thanks are extended to employees at Brno University of Technology and mainly in the international office for their help with scholarship documents.

My stay was financially supported by AKTION OeAD-GmbH and Erasmus+.

TABLE OF CONTENT

1 INTRODUCTION

Organic-inorganic hybrid materials are an interesting field of research and development as modern challenges and opportunities can be met by their emerging, novel properties and capabilities in various applications. There is a permanent demand to research and explore new structures and materials which possess additional properties that currently available materials are lacking. These ideas make such hybrid materials very attractive for an in-depth study of the system behavior. The structure is changed on a molecular level, and consequently materials properties can be tuned easily based on the composition.

Over the past few years, technological progress has increased and novel techniques for materials preparation have been developed and utilized in the industry as well. One of those methods is electrospinning for the preparation of fibers on the scale of micrometers down to tens of nanometers. This method has been known since the late 19th century but has received notable attention only recently and is becoming a viable technique for specialized applications. Nowadays, the electrospinning method is appreciated for its simplicity and versatility while techniques to improve yields are sought with appreciable effort. Electrospun fibers have found use in various sectors such as electronics, energy storage and conversion, environmental, catalysis, electronics, biomaterials and biomedical applications. [1] [2]

Organic-inorganic hybrid materials based on carbon-silicon networks are a novel class of materials which are intensively studied. These materials are investigated based on manifold chemical compositions and for a huge variety of different purposes. [3] However, electrospinning of such carbon-silicon materials has been rarely studied. [4] In principle and as a major advantage, the chemical variety of such hybrid structures allows for processing via various chemical reactions offering plenty of options. For example, sol-gel processing can be employed due to pendant reactive alkoxy groups, triethoxyphenylsilane is one example of that organic-inorganic hybrid material suitable for sol-gel processing and further electrospinning. [5]

1.1 Organic-inorganic hybrid materials

Organic-inorganic hybrid materials can provide unique and emerging properties that conventional materials and composites cannot. The phase behavior and interphase connectivity on the molecular level exert a dominant influence on the final properties. One of the present challenges is the synthesis of hybrid class II materials. This class is based on the combination of organic and inorganic components in a covalent rather than physical manner. Hybrid polymers represent a subclass and are based on inorganic building blocks and organic polymer segments covalently connected together. [6]

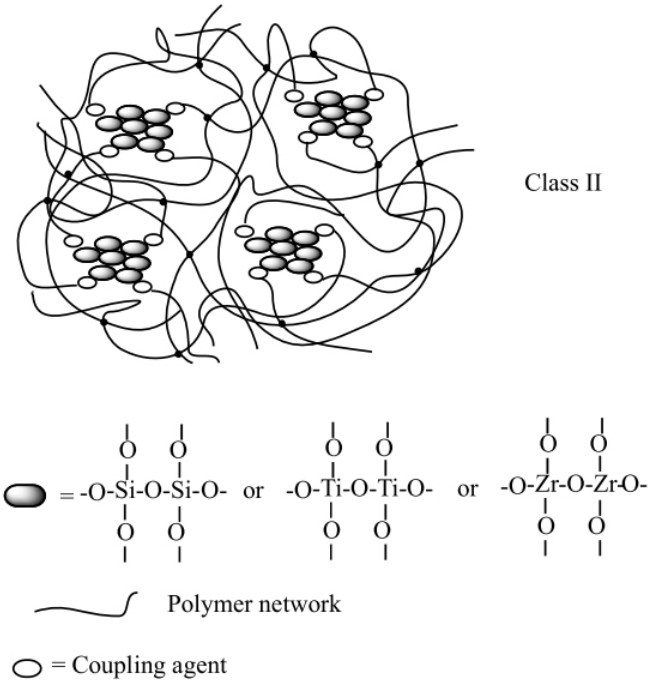

Figure 1: Representation of hybrid class II materials. Polymer forms covalent bonds between metal alkoxides such as silica, titania or zirconia via coupling agent or without if the polymer has pendant hydrolysable groups capable to form covalent bonds between the alkoxides. [7]

It is instructive to consider the structure of covalent co-networks of silica and organic polymers as an example of organic-inorganic hybrid material. Polymer chains are embedded in a continuous network of inorganic silica particles crosslinked by covalent bonds. Sol-gel processing in the presence of a coupling silane ($(RO)_3Si$-R') with R = methyl or ethyl and R' an organic functionality) can be employed to form such a co-network of silica and polymer. [6] A schematic representation of such a hybrid class II material is depicted in Figure 1; participating species undergo chemical reaction in order to form covalent bonds. For instance, compounds such as alkoxysilane-functionalized polymers can be transformed into a sol which contains pendant hydrolysable alkoxy groups serving as precursors capable of performing co-condensation and thus sol-gel processing. The transformation from sol to gel occurs and a three-dimensional (3D) network is formed. [8]

One of the advantages of hybrid organic-inorganic materials is the possibility to employ soft chemistry routes such as polymerization of alkoxide groups, encapsulation, templating and self-assembly approaches. [7] [9]

1.1.1 Alkoxysilanes

Many alkoxysilanes have been investigated in order to create organic-inorganic hybrid materials for various purposes and some were also examined towards their application in electrospinning. [5] [10] Alkoxy groups are capable to undergo hydrolysis and further

condensation reaction under appropriate conditions which makes alkoxysilanes the most prominent precursors for sol-gel processing. [11] These processes are described at length in Chapter 1.3. The condensation reaction leads to the formation of an interconnected 3D network that is filled with solvent. This network is also called a gel. [7] Some alkoxysilane precursors are carry functionalities that are capable –besides the hydrolysis and condensation reactions of the alkoxy moieties, to undergo polymerization reactions simultaneously under certain conditions. For instance, 3-glycidoxypropyltrimethoxysilane is capable of epoxy ring-opening polymerization while the alkoxygroups can undergo hydrolysis and condensation to form siloxane bridges. The organic polymer network is generated simultaneously with the formation of inorganic network. [12]

1.1.2 Polyorgano-silanes

Polymeric precursors of an organo-silicon nature (silicones or silsesquioxanes) have been recently studied regarding potential novel properties which can be obtained by thus prepared materials. As an example of that novel material is poly(methacryloxypropyltrimethoxysilane) which was used for gel preparation [8]. Although a vast array of different fibers has been already produced comprising organic polymers and polymer blends, there are few studies demonstrating electrospun fibers made from polyorganosilanes. The advantage of polyorganosilanes is the (pre)polymer structure representing a generally interesting feature. In terms of fiber formation by electrospinning the possibility of chain entanglements will have an impact on the spinnability of such polymer solutions. On the other hand, the nature of the polymer species with pendant alkoxygroups capable to undergo hydrolysis and condensation reactions can be used to obtain branched molecular structures from the linear chains. Of course, sol-gel processing can be engaged as well with the alkoxysilanes present on the chain and the functionalization of the chains or the network via this chemistry is accessible as well. [1] [4]

1.2 Free-radical polymerization

Polymerization is a process in which macromolecules are formed in a chemical reaction converting smaller units, typically monomers, into larger structures such as linear or branched chains, dendritic molecules or networks. If only one type of monomer is participating in the polymerization reaction, a homopolymer is formed where the monomer is representing the smallest molecular segment (repeating unit) in the macromolecule. The free-radical polymerization (FRP) is a chain growth polymerization in which the radicals represent the kinetic-chain carriers. Chain polymerization is characteristic for the reaction between monomer and active sites on the polymer chain resulting in a polymer chain. The growing chain is bearing an unpaired electron on one end. Reactive sites are regenerated at the end of each growth step. [13]

1.2.1 Reaction mechanism

The free-radical polymerization consists of three main steps:

The first step is the initiation reaction in which the radicals are formed. Addition of the initiator radical to one monomer occurs and as a result, the monomer is transformed into an active chain end while the initiator is added as the inactive chain end.

The second step is a propagation reaction where the chain is growing on the end which is bearing the radical. The propagation reaction proceeds by the radical attacking another monomer which is added, in turn, becoming the active chain end. Thus, successive addition of available monomers to the active macromolecular radicals at one end leads to a gradual chain elongation.

The third step is termination. The polymerization process is eventually slowed down and finished as no more additions of monomers are occurring. Termination reactions lead to the formation of unreactive stable compounds that cannot be activated by radicals again. For example, two radicals can react to form a covalent bond combining the two active species into an inactive combination of both. This process can occur between two active chains or one active chain and an active initiator. The latter type of termination is characteristic for highly concentrated initiator reactions or high viscosity polymerization solutions due to diffusion limits. The other possibility is termination by disproportionation reaction where one radical is transferred from one active molecule to the other, for instance by formal transfer of an elemental hydrogen. The result of this reaction is one unsaturated polymer chain which lost a hydrogen and a saturated polymer chain which accepted the hydrogen. [14]

1.2.2 Kinetics

The chain growth polymerization can proceed by two different types, either chain-growth or step-growth as is depicted in Figure 2. Conversion represents the fraction of monomer transformed into the polymer.

Chain-growth is characterized by a rapid increase in molecular weight at low degree of conversion, followed by an increasingly weak correlation to the degree of conversion. In the chain-growth polymerization, an active initiator is represented by a free-radical which can react with the functional group of a monomer typically a double or triple C-C bond. An active monomer then initiates a chain-reaction; in other words, the process proceeds with the addition of another monomeric unit to the activated monomer which, in turn, becomes the active site of the growing chain. Every active polymer chain has a defined lifetime before its growth is stopped by one or another termination event. A high number of active monomers is generated at roughly the same time at the start of the process and therefore rapid conversion of monomers into the polymer occurs. This is a reason for the high average molecular weight formation from the beginning of the polymerization reaction. The process of monomer addition is repeated, hence the propagation reaction is ongoing until all the monomer is depleted whereas the average

lifetime of the active chain largely determines the obtained average molecular weight. Chain-growth polymerizations are characteristic for short reaction times and low initiation temperatures. [14]

Step-growth polymerizations, on the other hand, are characteristic for a high dependence of molecular weight on the degree of conversion. As a result of the reactivity of the monomers, high molecular weight molecules are formed only at very high degrees of conversion. Monomer is available only at the beginning of the process and each individual molecule can undergo a polymerization reaction. Thus, step by step dimers, trimers, later oligomers are formed which can each react with another molecule to form a higher molecular weight product. As the reaction proceeds, the system gradually changes from monomers, to small oligomers and at high degrees of conversion longer and longer chains react to form even longer macromolecular products. The step-growth type polymerization is characteristic for long reaction times and high initiation temperatures. [14]

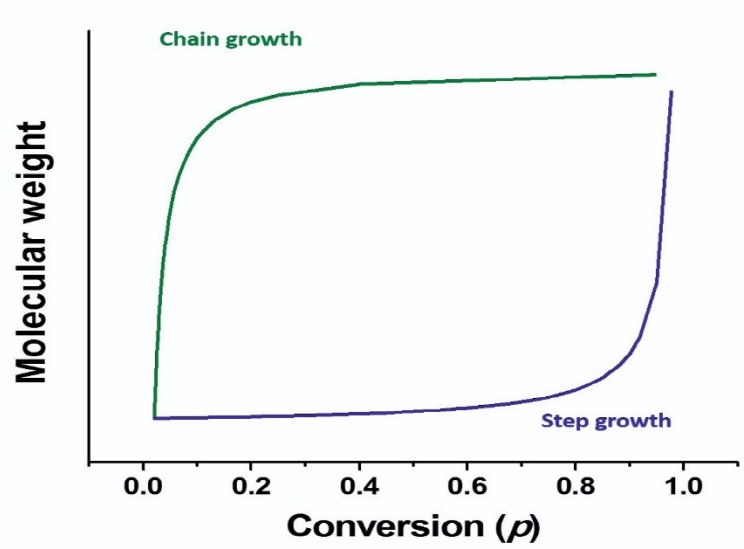

Figure 2: Dependence of molecular weight on the conversion with two dissimilar types of polymerization, either chain-growth or step-growth polymerization [15].

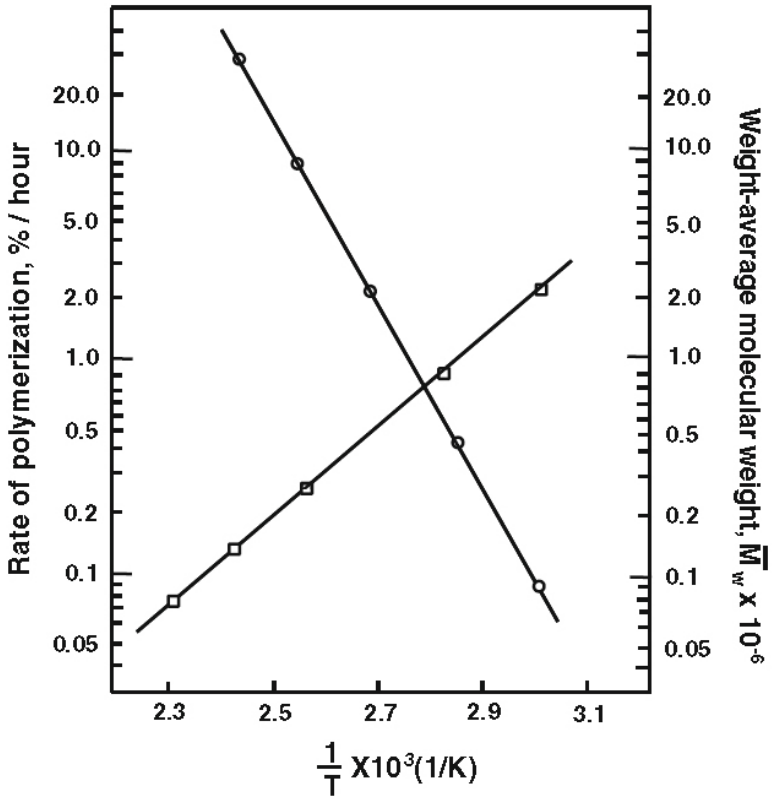

Figure 3: Dependence of the polymerization rate (circles) and molecular weight (squares) on the temperature. [14]

The rate of the polymerization is governed by the consumption of monomer. Initiator concentration and monomer concentration influence the overall rate of the free-radical polymerization. Increase of the initiator has an impact on increase of the polymerization rate. On the other hand, the polymerization temperature plays a major in resulting degree of polymerization and the reaction rate. Figure 3 shows dependence of rate of polymerization as well as the degree of polymerization on the temperature. As the temperature increases, the rate of the polymerization reaction increases but the degree of polymerization, represented by the weight-average molecular weight (M_w), decreases. [14]

1.2.3 Initiators

Radical polymerization is dependent on the formation of free-radicals which activate the monomer in the initiation step. Initiators decompose and form radicals under certain conditions. There are three major types of initiators dependent on the conditions necessary to induce initiator decomposition: thermal decomposition initiators such as peroxides and azo compounds, redox initiators and photoinitiators. [14] The thermal initiators will be discussed in more detail because they were utilized throughout this work.

Thermal initiators undergo homolytic dissociation above a certain temperature and generate radicals. The temperature employed for the decomposition influences the rate of radical formation while the initiator half-life is a parameter useful for the prediction of the dependence of reaction rate on the temperature. [14][16]

1.2.4 Bulk polymerization

Bulk polymerization is a polymerization technique and is characterized by its relative simplicity when employed at the laboratory scale while significant challenges are faced in the processes conducted at pilot or industrial scale. The polymerization is carried out in the presence of only monomer and initiator. Hence, it is a solvent-free reaction without any added contaminants usually yielding very pure product. However, the polymerizing product gets increasingly viscous during the synthesis which is reported as a disadvantage in the literature. One reason is the associated difficulty to control the temperature due to the exothermic nature of the polymerization reaction. Additionally, homogeneous mixing throughout the process is increasingly difficult due to the rising viscosity. [14]

1.3 Sol-gel processing

Sol-gel processing includes a transition between sol and gel. The sol is defined as a colloidal suspension of solid particles in a liquid and gel is a 3D network of these solid particles enclosing the liquid. The characteristic of the gel transition is an increase of viscosity due to formation of a 3D network, which enhances connections through the material. The most important chemical reactions during sol-gel processing are depicted in Figure 4. Formation of the gel is accomplished by concurrently occurring hydrolysis and condensation reactions. Metal and semimetal centers carrying alkoxy groups are in principle capable of these reactions, e.g. metal organic compounds such as tetraethylorthosilicate (TEOS) or the silsesquioxane hybrid materials as well. Here, it is instructive to consider the well-understood example of alkoxysilanes. The first step is the hydrolysis reaction where the alkoxy-silicon bond is cleaved by addition of water giving appropriate hydroxyls on the silicon as well as the released organic alcohol. In the second step, condensation reactions take place either between a hydroxyl and an alkoxy group or between two hydroxyl groups releasing either water or the appropriate alcohol. As a result siloxane bonds are formed between the two participating silane molecules. The alkoxy groups are consumed and later depleted for any other reaction, thus the system loses possibility for a second stage functionalization. E.g. postmodification of any materials resulting from sol-gel processing is not possible by further reactions of alkoxygroups. [17]

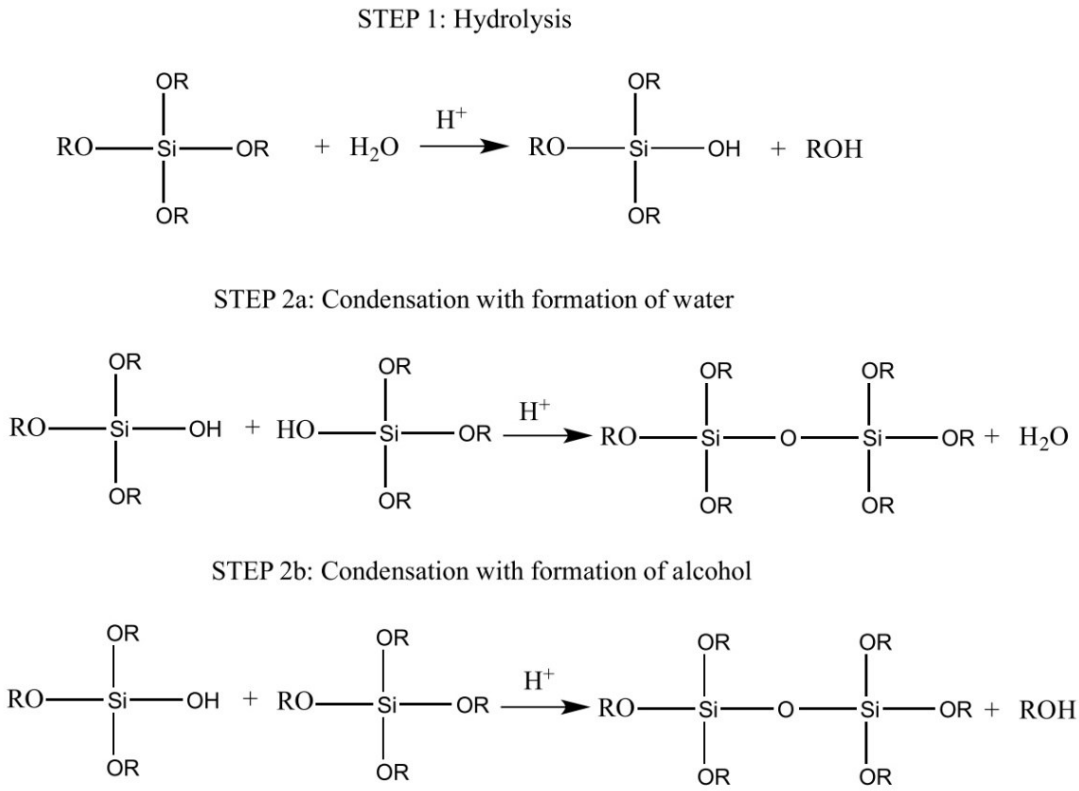

Figure 4: Sol-gel chemical reactions leading from sol to gel formation. Step 1: hydrolysis reaction of an alkoxysilane where R stands for an organic moiety of an alkoxy groups. Step 2a: Condensation reaction between two silanols. Step 2b: Another possible condensation route between a silanol group and a pendant alkoxygroup of a molecule in vicinity. [7]

The hydrolysis reaction is a nucleophilic substitution reaction of the alkoxygroup by a hydroxyl group. Water attacks the silicon atom and makes the silicon positively charged. Proton transfer occurs and generates an alcohol group as a better leaving group. Sol-gel processing leads to formation of cluster which are bonded to each other and form 3D polymeric networks so called gels. [18]

Catalysts can be utilized in the sol-gel processing in order to facilitate the hydrolysis and condensation reactions. Both are dependent on the pH of the surrounding environment as depicted in Figure 5. Therefore, acids or bases can be employed as catalysts. Between hydrolysis and condensation reactions competitive effects have to be considered.

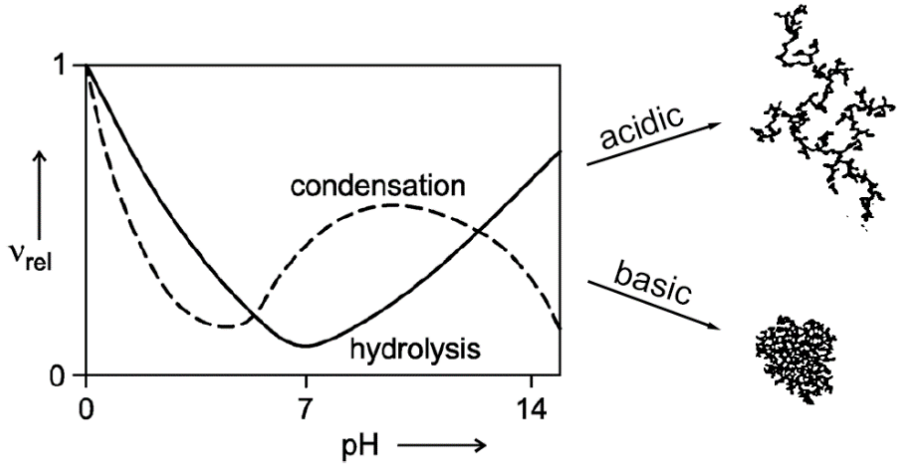

Figure 5: Dependence of hydrolysis and condensation rates upon the pH. The resulting structures of the 3D network are shown on the right side. The displayed curves represent the reactions of $Si(OR)_4$ as metal alkoxide precursor. The graphics was adopted from [17].

Under acidic conditions hydrolysis is faster than the condensation reaction, the latter one thus being the rate-determining step. First, the silanol is protonated fast and silicon becomes consequently more electrophilic and susceptible to attack by nucleophiles such as water or silanols. Protonated silanols preferentially condense with the least acidic silanol, which results in the formation of less branched clusters in an acidic medium. Therefore, the formed 3D network consists of more linear structures with a lower crosslinking density within the formed structures.

Under basic conditions, the hydrolysis is typically less favored and the condensation reaction is predominant, making hydrolysis the rate determining step. The condensation reaction under basic conditions rises to its maximum in relation to the simultaneous hydrolysis, as is depicted in Figure 5. The condensation begins with deprotonated silanols which preferentially attack the more acidic silanol groups. As a result, highly branched clusters are formed leading to larger particles in comparison to the acidic conditions. These clusters grow mainly by condensation reaction of hydrolyzed monomers. [17–19]

The kinetics of the sol-gel processes depend on more than one parameter: hydrolysis and condensation reactions are influenced by water/Si ratio, catalyst, and the nature of the silane. Temperature, pH, solvent, ionic strength, and silane/solvent ratio have an impact as well. Resulting gels can have either colloidal particle-like structure or are formed from sub colloidal chemical units forming a polymeric network. [19]

1.4 Electrospinning

The electrospinning method is based on the electrostatic attraction within the subjected solution and overcoming the capillary forces of a liquid during the electrospinning process. This process was first described in the 17th century and was further investigated on the basis of fluid droplet behavior in capillaries. Later on, these investigations were brought to the attention of Charles Vernon Boys who was the first to prepare fibers via the electrospinning technique in the 19th century. [2] Nowadays, the electrospinning process, also called electrostatic spinning, is well-studied, reasonably well understood and an established technique for industrial production of fibers of many kinds of materials including inorganic compounds such as metals, metal oxides (SiO_2, TiO_2, Al_2O_3), synthetic polymers (Nylon-6, poly(acrylonitrile), poly(propylene), poly(styrene), poly(vinylchloride), poly(vinylpyrrolidone) (PVP), poly(dimethylsilane)), biodegradable materials such as polylactic acid, but also natural polymers such as collagen, hyaluronic acid. [1] The technique provides a simple and versatile means to prepare continuous fibers with diameters ranging from the micrometer down to the low nanometer range. Many of current application such as filters, sensors, catalyst, biomedical materials were investigated in terms of electrospun fibers and an overview of studied sectors is depicted in Figure 6. [20] [21]

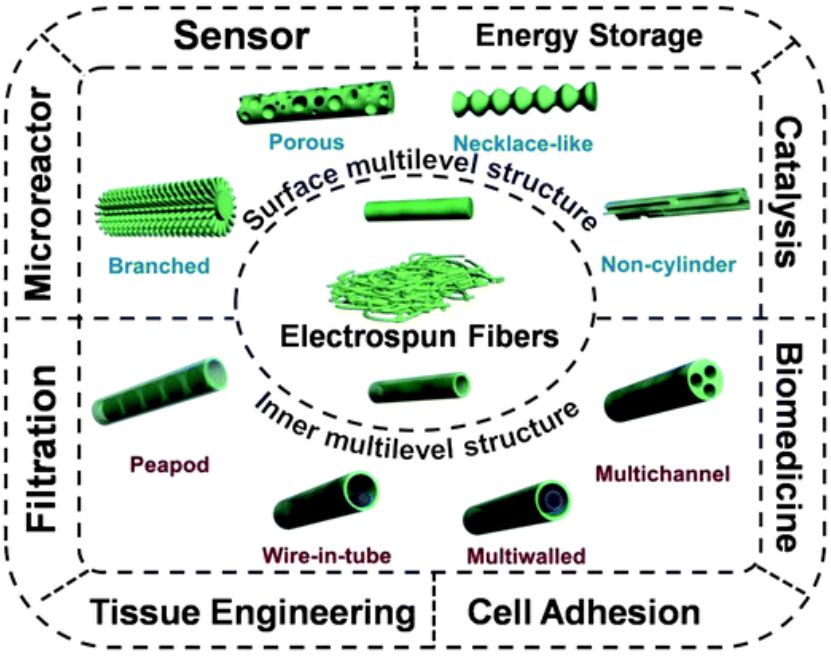

Figure 6: Overview of possible applications of electrospun fibers within various sectors. [21]

1.4.1 Principle of electrospinning

The fundamental principle of the electrospinning technique is entirely physical. Fibers are formed due to the presence of an electrical field between two electrodes where the solution is essentially drawn in the form of an elongated stream from one to the other. [1] The electrospinning device includes a high-voltage power supply, a syringe pump, a spinneret represented by needles in many cases and a conductive collector. The power supply can either provide direct (DC) or alternating current (AC). The technique is based on application of a high voltage to a capillary filled with the solution and collecting the fibers on the grounded collector in a certain distance from the capillary. [2] During the electrospinning procedure, the liquid is fed through the spinneret at a constant feed rate by the syringe pump. Electrospun fibers of different diameters as well as various morphologies can be produced depending on the process conditions such as the voltage, flow rate, diameter of spinneret and tip to collector distance. [1]

The procedure of fiber formation in detail is as follows: the liquid is extruded from the tip of needle where the liquid forms a droplet. Since the liquid is exposed to an electric field, charges within the liquid experience a force, accumulate at the droplet surface and the droplet is deformed into a so-called Taylor cone. The electrostatic force exerted on the fluid overcomes the surface tension and fluid is ejected towards the nearest point of the opposing electrode, which is the grounded collector. The fluid stream migrating toward the collector due to electrical field effectively closes the circuit and, given appropriate conditions are met, the liquid exits the droplet in the form of a continuous stream. The liquid jet then quickly evaporates during flight due to the high surface to volume ratio. However, if the liquid was carrying a polymer, solid fibers (more or less dry) are obtained, which form a non-woven mat on the target surface. A scheme of these events and the electrospinning process is depicted in Figure 7.

Electrospinning begins with droplets changing into a Taylor cone and a jet which is ejected towards a collector. The conical shape of the jet can be maintained as long as a sufficient amount of the liquid is constantly provided to replace the ejected amount during the electrospinning process. [1]

The droplet shape changes into a Taylor cone upon application of the high voltage when the electric field overcomes a critical value of the electrical forces beyond the surface tension of the droplet. The jet is subjected to drag forces such as electrostatic force, drag force, gravity, Coulombic repulsion, surface tension, viscoelastic forces, which compete with the electrical force necessary for the fluid stream formation. When the fluid stream is ejected by the electrostatic force from the tip of needle towards the collector, a drag force is introduced as a result of the jet and surrounding air interaction. Expansion of the droplet is ascribed to Coulombic forces and contraction is attributed to a surface tension and viscoelastic forces. An applied electric potential resulting in an electric field influences the electrostatic and Coulombic repulsion forces observed during the process. [22]

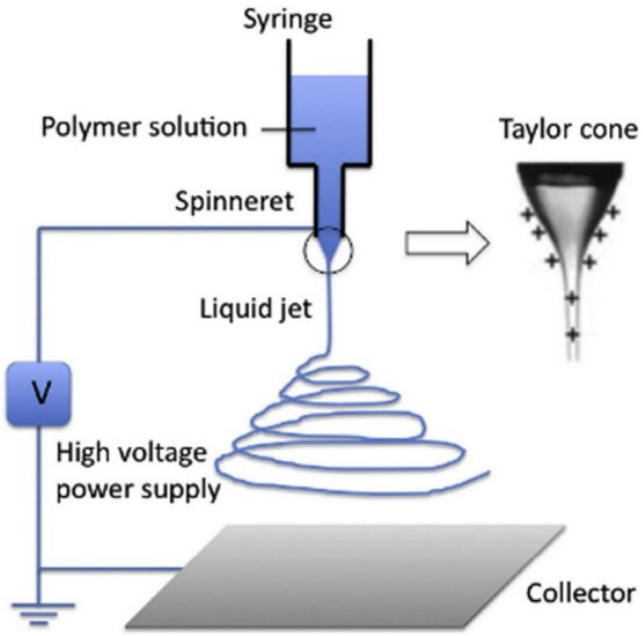

Figure 7: Scheme of the electrospinning process. The usual set-up consists of syringe with an electrospinning solution (such as polymer solution) which is fed through the spinneret. Upon applying of the high voltage to the spinneret, the Taylor cone is formed. Charges accumulate on the surface of the Taylor cone as well as along the liquid jet which is drawn to the grounded collector. [22]

The electrically charged jet is ejected and accelerated by the electric field to the collector. Several models can be used to describe the jet during electrospinning process, such as a straight string of connected and viscoelastic dumbbells or the other model describes a long and slender stream. In a general procedure, the driven jet can be described as follows: At the beginning, the tapered jet follows a straight line for a certain distance from the tip of the spinneret. This distance is called the near-field region. The Rayleigh instability can cause a break of the jet and therefore the viscoelastic properties of the solution have to suppress this phenomenon. The surface charges align along the jet and generate a flowing current. [1] Then, the helical path is formed as a result of bending instability and the distance is called far-field. Repulsive forces along the jet cause repulsions of the jet segments and effect these segments to force upward and outward from the straight segment. [23] Bead-like fibers can be formed if the density of charges carried on the jet is reduced and therefore the capillary instability can cause a disruption into droplets leading to the formation of beaded fibers. During the elongation, the jet is getting thinner in diameter and solvent evaporates so the fiber is getting less flexible. It results in a change of the volume and viscoelasticity of the jet during the electrospinning until the fiber solidifies and hits the collector. As a last step, fibers are deposited on the grounded collector and a nonwoven mat of fibers is created. [1]

The charges stay on the surface of the dried fibers until the fibers are deposited on the grounded collector. However, many deposited materials show a low conductivity and measurable amounts of residual charges still remain on the fiber surface. [1]

1.4.2 Processing conditions

The electrospinning process can be generally controlled by changing the electrospinning setting and solution parameters, which have profound impact on the ability to form fibers in the first place and also the structure of electrospun fibers. Furthermore, the fiber formation is affected by processing parameters such as the applied voltage and the feed rate of the solution. Setup parameters such as spinneret to collector distance and spinneret inner diameter have an impact on fiber formation as well. Ambient parameters such as temperature, humidity and air velocity in the processing chamber also play an important role. As mentioned above, solution parameters are another important feature since the composition of the solution and its physical properties affect the fibers. [24]

A successful formation of fibers originates from adjusting process and system (solution) parameters in just the right way. It is necessary to optimize all the processing parameters in order to achieve stable fiber formation and control of the electrospinning process. For example, the applied voltage determines the amount of charges on the surface of the droplet and later on the jet. [1] The distance of spinneret and collector mainly affects the morphology of the electrospun fibers so that a beaded fiber structure is, for instance, mainly caused by high voltage and distance to the collector. [24]

In some cases, the jet is interrupted resulting in the formation of fine droplets which repel each other due to electrostatic effects. The transition between this phenomenon called electrospraying and electrospinning of continuous fibers is mainly governed by the properties of the liquid such as viscosity and viscoelasticity, surface tension and ionic conductivity and proceeds via a combination of both, resulting in so called beaded fibers. Another parameter that is vital for the process is related to the nature of the polymer and its concentration is the average number of entanglements with neighboring macromolecules per polymer chain [22]. Although not desirable in terms of fiber formation, electrospraying is used by ion mass spectroscopy for the electrostatic atomization of liquids. Another application of electrospraying is the preparation of particles for various applications such as biomedical, size particle fabrication or photovoltaics. [25]

2 IMPORTANT CONCEPTS

Organic-inorganic hybrid materials have recently entered the research field of electrospinning. Various materials have been tested for fiber preparation via electrospinning based on hybrid polymers as well as the sol-gel process. [1, 5, 10] Generally speaking, polyorgano-silanes as promising materials for various uses have been mainly applied for the preparation of aerogels with unparalleled functionality. [3] Since the present work aims to combine these two concepts, the following chapter introduces some of the latest research done in those fields as well as some important basic concepts used throughout the thesis.

2.1 Radical polymerization of organo-silanes

Polyorganosilanes are organic-inorganic materials which consist of a carbon based polymer backbone with pendant inorganic side groups comprising silicon. [13] The side group is an alkoxysilane group which can undergo hydrolysis and condensation reactions under certain conditions. [26]

Free-radical bulk polymerization with the use of a thermal initiator is one of the recent approaches in terms of obtaining polyorgano-silanes polymerized via a vinyl group. Kanamori et al. studied this polymerization in order to achieve polymers of various molecular weights for further aerogel preparation. Di-*tert*-butyl peroxide (DTBP) was utilized as a thermal initiator. Several different vinylalkoxysilane monomers were studied: specifically vinylmethyldimethoxysilane (VMDMS), vinyldimethylmethoxysilane, vinyltrimethoxysilane, vinyltriethoxysilane, allyltrimethoxysilane, allyltriethoxysilane, allylmethyldimethoxysilane. [27] [28] According to the M_w analyzed by size-exclusion chromatography (SEC) for the reported poly(vinylmethyldimethoxysilane) (PVMDMS), the size is almost constant with polymerization time and increases with initiator concentration as shown in Table 1.

Table 1: Kanamori PVMDMS results for M_w regarding to initiator concentration and polymerization time dependence. Adopted from the literature [29].

DTBP [mol.%]	**Polymerization time** [hr]	M_w [g/mol]	**Conversion** [%]
1	24	5 358	91
1	48	5 356	95
1	72	6 038	99
5	48	8 998	99

Table 2: Half-life of the DTBP upon various decomposition temperatures [14].

Temperature [°C]	**Half-life** [hr]
100	218.0
115	34.0
130	6.4
145	1.4

Table 2 shows the dependence of DTBP half-life with respect to temperature. According to the literature, the decomposition temperatures of DTBP usually employed are in the range of 120–140 °C in order to achieve an optimum polymerization temperature and radical formation efficiency. However, it is important to consider that the half-life of DTBP is changing with the decomposition temperature and therefore has an impact on the polymerization rate. [14]

The polymerization of vinylalkoxysilanes is obviously not common and has therefore not been well examined until now. The mechanism of the free-radical polymerization of vinylalkoxysilanes has not been fully elaborated in terms of experimental data. However, some studies of chain transfer with monomer and polymer in a bulk FRP have been reported in the literature. [30]

2.2 Electrospinning of hybrid materials

Organic-inorganic materials such as organosilanes have already been investigated for the formation of functional fibers and the procedure included sol-gel processing in order to achieve polymeric structures by reaction of alkoxysilane groups. Hence, the spinnability was increased by the formation of polymerized networks in the material prior to electrospinning. Solution properties had to be carefully adjusted for successful fiber formation applying electrospinning. [10] [5] However, a possibly superior approach is to employ an already formed polymeric structure, e.g. polyorganosilanes achieved by polymerization, with inherent spinnability to keep the side groups available for further reactions and post-spinning modifications.

2.2.1 Electrospun alkoxysilanes

Alkoxysilanes have been intensively studied in terms of electrospinning and it has always involved the sol-gel processing to obtain an interconnected structure. Electrospun fibers consist of either nanoparticles merged together resulting in rugged or thin fibers. [31] [32] Hydrolysable species can be employed as coupling agents to covalently connect the inorganic parts of the network with organic molecules resulting in the formation of an interconnected network. The interface between the organic and inorganic parts is created as a consequence of

these reactions. Various inorganic species such as alkoxysilanes and other metal alkoxide materials such as silica, alumina, titania, vanadia can be connected with organic polymers via the sol-gel processing approach outlined above. [7] [33] As an example, silica particles can form a 3D network by interconnecting silane coupling agents. [34] [31]

TEOS as an alkoxysilane precursor has been the best investigated precursor for sol-gel based materials to produce fibers by the electrospinning process. Geltmeyer et al. studied the effects on the electrospinning process in terms of the sol viscosity, concentration of the precursor and the degree of crosslinking, as well as the size of the resulting colloidal particles. They reported that there is a viscosity dependence on the other three parameters. Thus, the stability of the jet formation, the droplet and bead-like structure formation and the diameter of the electrospun fibers can be tuned by change of the solution viscosity. The electrospinning process was stable and reproducible in terms of fiber formation in certain ranges of viscosity values for the investigated TEOS system. Outside of the stable region, beaded fibers were formed or the electrospinning process was not stable due to the jet break-up and resulted in electrospraying or droplet formation. [10]

Holubová et al. studied fibers made of TEOS and coupling agents, namely triethoxyphenylsilane and 1,4-bis(triethoxysilyl) benzene. Spinnable solutions were prepared with both coupling agents and gelation times differed due to the different amount of alkoxygroups on the coupling agent species, e.g. double amount of alkoxygroups on 1,4-bis(triethoxysilyl) benzene resulted in faster gelation. The key factor was to adjust hydrolysis and condensation reactions, as well as to overcome premature gelation in order to achieve successful electrospinning. The hydrolysis reaction has to be suppressed with respect to the condensation reaction because then the network can branch slowly but still increase the polysiloxane structure and thus result in higher viscosity without premature gelation. In terms of electrospinning of sol gel materials the most suitable structure seems to be a ladder-like weakly branched organosilane structure. [5]

Interestingly, from the approaches reported so far in the literature one obvious strategy is apparently lacking entirely: The use of prepolymerized organosilanes in a sol-gel manner in order to obtain solutions suitable for the electrospinning of organic-inorganic hybrid nanofibers.

2.2.2 Electrospun polyorgano-silanes

As an example of polyorganosilanes fibers, poly[styrene-co-3-(trimethoxysilyl)propyl-methacrylate] can be highlighted in terms of electrospun fibers. Xu et al. performed a study on this polymer as a novel organic-inorganic hybrid material from which fibers were prepared via electrospinning. Thus obtained fibers showed a smooth and uniform surface and reproducible diameter. Sol-gel processing of the pendant trimethoxysilyl groups was investigated later on, as a post-process after electrospinning and resulted in remarkably enhanced solvent and temperature resistance of thereby treated fibers. [4]

Nevertheless, there are no available studies on the application of polyvinylsilanes in terms of electrospinning and sol-gel processing. The polyorganosilane materials were however studied in detail with respect to sol-gel processing for aerogel preparation by Kanamori and Nakanishi. Allylalkoxysilanes and vinylalkoxysilanes were investigated in order to achieve polymeric precursors for further sol-gel processing towards aerogel preparation. [3] [35] A similar approach for the preparation of aerogels based on the vinyltrimethoxysilane was utilized by Rezaei et al. The sol-gel reaction and also the resulting 3D structure can be tuned by the solution composition. [36]

2.3 Polymer solution characteristics for electrospinning

A wide range of investigations on polymer solutions for electrospinning has been published in the literature, including synthetic and biopolymers. [1] The system properties in terms of the solution are of great importance because they not only influence the diameter and the morphology of the electrospun fibers such as particle, bead-like or linear fiber structure, but most importantly the ability to form fibers in the first place. Molecular weight, molecular-weight distribution and architecture of the polymer has an impact on the solution properties such as viscosity, conductivity and surface tension and therefore also governs the ability to form fibers. [22]

2.3.1 Polymer solution properties

The structure of electrospun fibers can be altered by properties of the spinning solution including concentration, solvents and loading with various precursors, type of monomer or additives. [1] A beaded structure of electrospun fibers is mainly influenced by surface tension and conductivity of the solution. [37] The nature of the polymer is one of the main parameters influencing fiber diameter and morphology. [22] Porosity and bead formation are also governed by the concentration of the polymer and the properties of the solvent because they have an effect on viscosity and surface tension of the solution. [38]

2.3.2 Molecular weight of polymer

Physical properties of the electrospinning solutions are mainly governed by the molecular weight of the polymer. For example, molecular weight of the polymer influences viscosity and viscoelastic properties of the polymer solution. An important parameter for a spinnable polymer solution related to molecular weight is the average number of chain entanglements of each individual macromolecule. These entanglements can be viewed as physical overlaps between

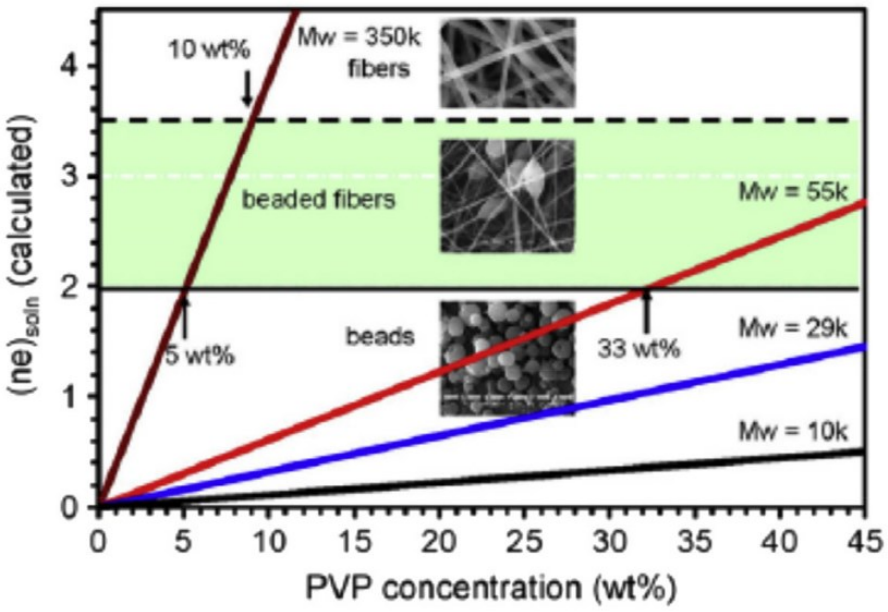

Figure 8: The chart displays polymer entanglements as a function of polymer concentration, polyvinylpyrrolidone varying in molecular weight, specifically. Inserted SEM pictures show structure of final particles or fibers in certain entanglement region. (Munir et al. 2009)

polymer chains restricting the movement of the individual chain in solution and they depend on the shape, size and concentration of the polymer. [39] An insight into the entanglements gives a theory about reptation of a polymer chain described by Gennes. Polymer chains exhibit a continual stochastic motion in the solution due to the chain mobility and diffusion. Entanglements are represented by a transient network of a freely jointed chains and have a significant dependence on the molecular weight. [40]

There are three main regimes which have to be considered in terms of polymer chain entanglement and the resulting fibers. These regimes are depicted in Figure 8. Formation of fiber structure depends on the polymer concentration due to formation of polymer chain entanglements in the electrospinning solution. [41] And hence, dependent on the number of chain entanglements, smooth fibers, beaded fibers or particle-like structures can be formed. More polymer entanglements result in a higher probability of smooth fiber formation without defects. Additionally, below certain molecular weights, fibers cannot be formed because the system favors particle-like structure due to insufficient chain entanglement. [42] [39]

2.3.3 Impact of solvent

Another important parameter is the choice of solvent for electrospinning because it has an effect on conductivity, viscosity and surface tension of the electrospinning solution not to mention the effects on the polymer behavior in solution and the resulting change in entanglement behavior. Furthermore, the volatility of the solvent must be considered for the electrospinning process

since the solution properties can thereby be changed substantially at the surface with respect to the bulk liquid.

Li et al. studied effects of various solvents in regard to the electrospinning process of polymethylmethacrylate (PMMA) where dichloromethane, acetone, chloroform, tetrahydrofuran, ethyl acetate, dimethylformamide were characterized in terms of the effect on the hierarchical structure and morphology of the formed fibers. Naturally, surface tension, conductivity and viscosity of the solution are affected by the choice of solvent and are of great importance for the fiber structure (smooth or bead like). Differences in volatility determine evaporation rates of the solvent and thus drying time of the fibers during flight. The concentration of the polymer in the spinning solution has to be considered to maintain a stable jet. As a result, the solvent itself does not have the most significant impact on the fiber structure because it is mainly dependent on the nature of polymer and its concentration. However, as mentioned above, the conformation of the macromolecules in solution can be significantly different and therefore influence the ability to obtain spinnable solutions. Furthermore, solvents can induce and affect pore formation processes due to vapor-induced phase separation at the surface which is caused by different evaporation rates of solvents. [43] As the concentration of solvent changes in proximity of the solvent-air interface, the system enters the meta- or unstable region inducing phase separation. Solvent or polymer rich domains start to form, which result in the formation of pores. [38]

Zuo et al. reported the influence of solvents on the poly(hydroxybutyrate-co-valerate) fiber morphology. Polar and non-polar solvents, as well as their mixtures were studied in relation to the conductivity of electrospinning solution. Alcohol mixtures favored formation of non-beaded fibers. Moreover, surface tension was examined as another solution parameter for deeper insight into the impact of the solvent. Higher surface tension of solutions correlated with bead-like structure of fibers as the formation of beads was probably caused by the favorable surface to volume ratio with respect to the fiber structure and consequently a decrease in the free energy of the system. [44]

3 RESEARCH OBJECTIVES

The overall aim of this thesis is the preparation of polyvinylsiloxane based nanofibers using poly(vinylmethyldimethoxysilane). Composites consisting of condensed PVMDMS belong to class II hybrid materials based on silanes where the organic and inorganic parts are connected by covalent chemical bonds. Resulting crosslinked structures are called polysiloxanes but in general in the literature these networks are referred as hybrid silica. [6] PVMDMS is described in the literature, however, it has not been studied in the connection with electrospinning or fiber formation so far. [3] [29] Therefore, the major challenge of this thesis is to find suitable reaction conditions and solution properties for electrospinning. To achieve this, a careful adjustment of the precursor structure, the spinning solution properties, and the electrospinning processing conditions has to be performed. Figure 9 depicts a schematic approach used for accomplishing the aim of the project.

First, the precursor molecule polymerized VMDMS is prepared and characterized in detail; second, electrospinning parameters such as initiator concentration, are investigated to generate stable PVMDMS fibers and third, crosslinking the PVMDMS by processing the precursor under sol-gel conditions. The latter approach is necessary because PVMDMS results in silicone like structure which is non-covalently intermolecularly interacting only by entanglement of the polymer chains. More stable materials should be obtained by generating a 3D connectivity.

Successful electrospinning is achieved by set of the solution parameters such as molecular weight and polymer concentration. PVMDMS has to be investigated in regard to the electrospinning process. The radical polymerization used throughout the project was inspired by the work of Kanamori et al. [29]

The electrospinning technique is used as a method to produce fibers. There are plenty of publications on electrospinning of polymers and some of them cover also similar materials,

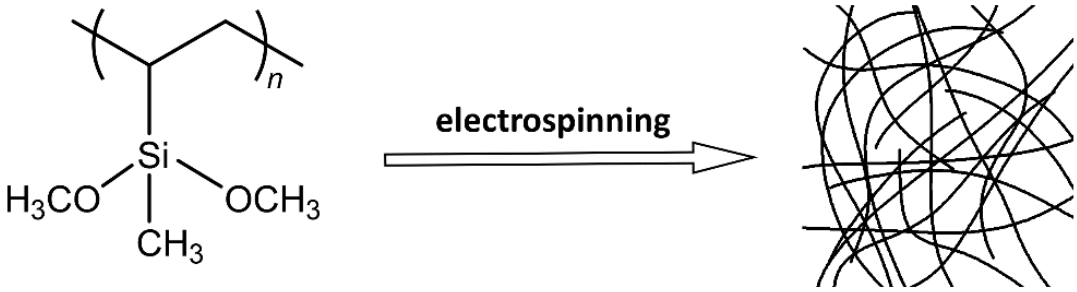

Figure 9: Schematic illustration of the electrospinning approach using PVMDMS.

however using VMDMS and the corresponding polymer represents a complete unknown approach. It is well known that the electrospinning process is influenced by the molecular weight of the polymer as well as its concentration in the solution. Therefore, the main focus was set to studies of the influence of these parameters. Furthermore, approaches in this project were the electrospinning of polymer blends of PVMDMS and PVP, the latter one often being used to positively influence electrospinning processes.

Another approach to produce stable fibers based on the used polymer is the investigation of sol-gel processing prior to electrospinning. The investigation aims to determine influence on the electrospinning technique since prediction of the crosslinking should have a positive effect on the spinnability of this precursor due to transition form 2D to 3D network. Therefore, the acidic environment for catalytic reaction is studied in this thesis and in the same time influence of water to the hydrolysis and condensation reaction.

To summarize, the tasks of aimed objectives are summed up in the following:

- Investigation of the ability to prepare fibers from the synthetized polymers based on VMDMS in terms of:
  - solution properties of PVMDMS under different polymerization conditions,
  - usage of carrier polymer,
  - sol-gel process conditions.

4 EXPERIMENTAL

4.1 Chemicals

Vinylmethyldimethoxysilane (97%, *Abcr GmbH*). Di-*tert*-butyl peroxide (≥98.0%). Methanol (dry, 99.8%, *Alfa Aesar Thermofisher GmbH*). Polyvinylpyrrolidone (M_w = 1.3 MDa, *Sigma Aldrich*). Hydrochloric acid (32%, *Merck KGaA*). Methanol-D4 (99.8 at-%D, *ARMAR Chemicals*). All chemicals were used as received without any further purification. Reactions in aqueous solutions were carried out using *Milli-Q* water with a resistivity higher than 11.8 MΩ·cm at 25 °C.

4.2 Instruments

Polymerization reactions. A hydrothermal reactor with connected thermostat control was used to carry out the polymerization reactions. The reaction vessel was made of teflon and the volume was 200 mL. The set-up is depicted in Figure 10.

Figure 10: The hydrothermal reactor with heating and stirring plate is shown on the left side, the thermostat control unit for the reactor is depicted on the right side.

Electrospinning. The electrospinning instrument was provided by *LINARY NanoTech* company and was composed of digitally controlled syringe pump to provide constant feed rate, high voltage power supply to provide high voltage and collector of dimension 20 × 30 for an accumulation of fibers. Used needle was a blunt type of diameter 21G and dimensions 0.80 × 22 mm. Detail description of the device and its components is shown in Figure 11.

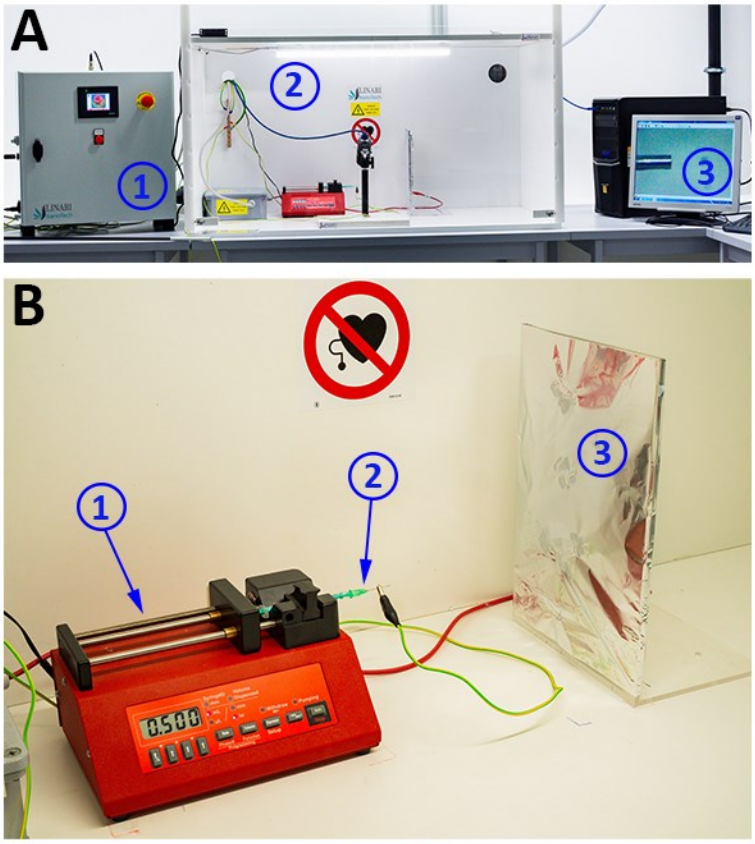

Figure 11: Part A depicts the whole electrospinning apparatus, 1 – high voltage power supply, 2 – electrospinning hood, 3 – computer and monitor. Part B illustrates in detail the parts in electrospinning hood; 1 – digitally controlled syringe pump, 2 – syringe and needle, 3 – collector covered by aluminum foil, respectively.

Optical microscope. Zeiss Axio Imager.M2m equipped with EC Epiplan-NEOFLUAR objectives was used to capture images of electrospun fibers.

FT-IR. The Fourier transform infrared spectroscopy (FT-IR) was carried out on the instrument *Vertex 70* from *Bruker* with the platinum-attenuated total reflectance module. Simulation of molecular model of PVMDMS was performed and peak intensities were calculated by MOLDEN.

DLS. Size distribution measurements by dynamic light scattering (DLS) were carried out on the device *Zetasizer Nano ZSP* delivered by *Malvern*. Cuvettes used for all the experiments

were made of PMMA and were semi-micro type obtained from *Brand*. Measurements were carried out at 25 °C. The solutions were filtered prior to the measurement, filtration paper of density 87 g/m^2 and grade 292, *Sartorius^{TM}* was used. The used software was *Malvern Panalytical* version 7.03. Final value of z-average was evaluated by the software and values far from the trend were excluded for further data processing.

NMR. Nuclear magnetic resonance (NMR) was employed in order to determine number-average molecular weight (M_n) of polymers and the analysis was performed on a 600 MHz *Bruker Avance III HD* spectrometer equipped with a ^{1}H/^{13}C/^{15}N/^{31}P quadruple-resonance probe spectra were recorded at 298 K in 5 mm NMR tubes (*ARMAR*, Type 5TA). The following experiments were recorded: 1D-^{1}H, 1H–^{13}C HSQC and ^{1}H–^{1}H NOESY. The proton signals of H-atoms located at the CH_3 (Signal b) were compared with the CH_3 groups (Signal a_1+a_2) using a ^{1}H–^{13}C HSQC spectrum (relaxation delay: 15 s, NS: 20, DS: 256). For data processing and analysis, integration and signal-to-noise (S/N) determination, *Topspin* 3.5/3.6 (*Bruker*) and *Sparky* 3.114 (T. D. Goddard and D. G. Kneller, SPARKY 3, University of California, San Francisco, USA) by using standard protocols were used, respectively.

4.3 Free-radical polymerization of VMDMS

Bulk FRP of VMDMS were carried out in a hydrothermal reactor. The reaction is schematically depicted in Figure 12. The reaction procedure was based on the results of Kanamori et al. [3] The overall mechanism of the FRP including formation of *tert*-butoxy and methyl radicals is shown in Figure 13 and was useful in order to assign peaks in the NMR analysis regarding to the chain end-groups.

In the general procedure 15 mL of VMDMS and specific ratios of DTBP as radical starter were charged and mixed in the hydrothermal reactor. The amount of DTBP was varied between 1–30 mol%. After being flushed with Ar, the reactor was sealed and then heated at 120 °C for 18 to 72 hr and stirred at 375 rpm to promote FRP of the monomer. After cooling down to room temperature a transparent viscous liquid (l) or solid (s) was obtained containing PVMDMS.

Table 3 gives an overview of the synthetized polymers during the project. It shows specific ratios of the radical starter to monomer used during polymerizations and times of reaction. Sample labeling used throughout the project follows shortcut KSH-initiator amount-duration of polymerization.

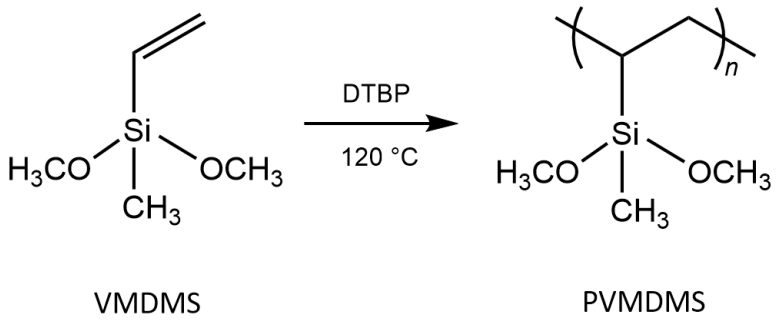

Figure 12: Radical polymerization reaction of monomer VMDMS with DTBP as an initiator.

Table 3: Details of prepared polymers based on the initiator concentration during the synthesis and resulting texture of the polymer. Texture symbol l stands for liquid appearance of the polymer and s for solid.

Sample label	**DTBP/VMDMS** [mol/mol %]	**Duration** [hr]	**Texture**
KSH1-48	1.0	48	l
KSH3-48	3.0	48	l
KSH4-48	4.0	48	l
KSH5-48	5.0	48	l
KSH10-48	10.0	48	l
KSH10-72	10.0	72	l
KSH11-48	11.0	48	s
KSH12.5-48	12.5	48	s
KSH15-72	15.0	72	s
KSH20-48	20.0	48	s
KSH30-18	30.0	18	s
KSH30-18.5	30.0	18.5	s

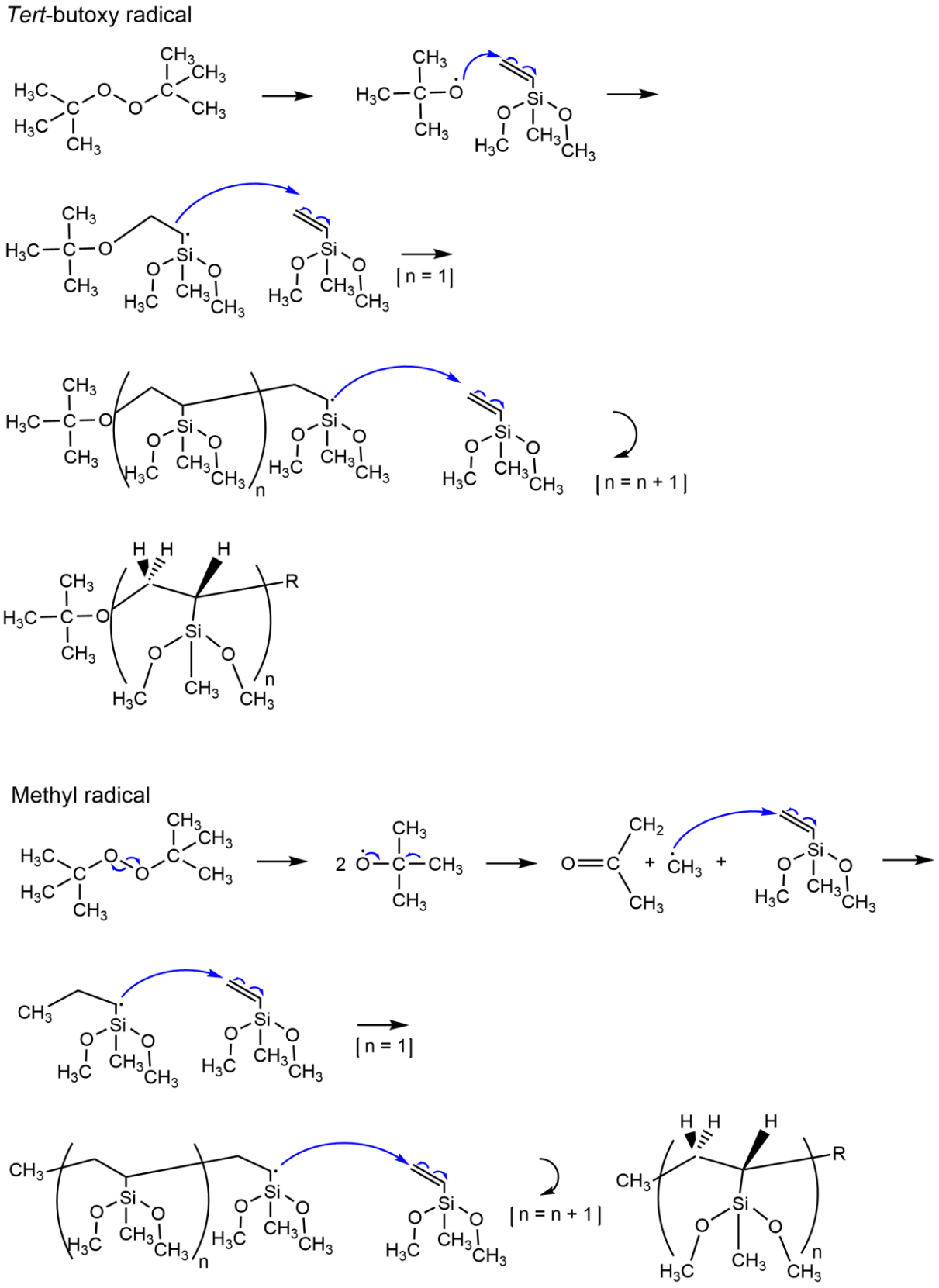

Figure 13: Overall mechanism of the FRP involving radical formation.
The reactions depict the end-groups of the chains, either *tert*-butoxy or methyl. The reactions were remade based on the literature. [45]

4.4 Preparation of PVMDMS solutions

Synthetized PVMDMS was weighted and the solvent methanol (MeOH) was added to prepare polymer containing solutions for the electrospinning process. Liquid polymerization products, specifically KSH1, KSH3, KSH4, KSH5, KSH10 were dissolved in MeOH at ambient conditions under stirring. Solid polymers, specifically KSH11, KSH12.5, KSH15, KSH20, KSH30 were dissolved in MeOH up to 50 wt.% under stirring at 55 °C until the solution was transparent and homogeneous. Polymer solutions of concentrations above 50 wt.% were prepared by evaporation of MeOH under reduced pressure. Polymer solutions were also subjected to sol-gel processing.

For NMR sample preparation, KSH-1-48, KSH-5-48 and KSH-10-48 were dissolved in methanol-D4 and measured immediately after preparation. Insoluble polymer, like KSH-30-18 was additionally stirred at 50 °C for 48 hr.

4.5 Polymer size distribution analysis

Solutions of PVMDMS in MeOH of various molecular weights and of 5–36 wt.% concentration were prepared for the particle size measurements, the measure z-average of polymer in solution was evaluated by the Malvern Panalytical software based on the obtained data. Table 4 shows investigated samples for DLS measurement of polymer z-average in MeOH.

Cuvettes used for all the experiments were made of PMMA and were semi-micro type obtained from *Brand*. The solutions were filtered prior to measurement, filtration paper of density 87 g/m^2 and grade 292, *Sartorius*^{TM} was used.

Table 4: PVMDMS solution in MeOH for DLS measurement.

Polymer PVMDMS	[wt.%]	**Polymer PVMDMS**	[wt.%]
KSH1-48	5	KSH10-48	5
KSH1-48	12	KSH10-48	12
KSH1-48	25	KSH10-72	5
KSH1-48	36	KSH11-48	5
KSH2-48	5	KSH12.5-48	5
KSH3-48	5	KSH15-72	5
KSH3-48	12	KSH20-48	5
KSH5-48	5	KSH30-18	5
KSH5-48	6	KSH30-18	10
KSH5-48	12		

4.6 Sol-gel processing

Sol-gel processing of prepolymerized PVMDMS was studied. The reactions during sol-gel processing in the studied PVMDMS system are schematically depicted in Figure 14. Sample preparation is based on a two-part reaction mixture system.

The first part is an acidic solution and the second is a polymeric solution. The acidic solutions were prepared using HCl, water and MeOH. Specific amounts of concentrated HCl (32%) were added into a mixture of DI water and dry MeOH in order to obtain solutions with pH values ranging from 1 to 6. The final pH in the combined solution, after addition of acidic solution into polymeric solution, is used throughout the project to describe the system. The water to monomer molar ratio is calculated based on the amount of water in the aqueous acid solution and the content of PVMDMS in the final solution and this ratio was set between 1–6 mol/mol. Shortcut *R* was used for molar ratio water to silane (H_2O/Si) throughout the project in order to label samples. Sample labeling was as follows for sol-gel processing: KSH-initiator amount-duration of polymerization-weight concentration of PVMDMS in starting solution. Used ratios of prepared solutions are given in Table 5.

To investigate the gelation behavior of PVMDMS solutions in MeOH, the prepared reaction mixtures were poured into plastic containers and the appropriate amount of acidic MeOH solution was added to adjust a certain pH value and a H_2O/Si molar ratio. The solution was then stirred for approximately 15 min and was aged at ambient conditions to determine the gelation time.

Reaction mixtures that were subjected to the electrospinning process were prepared in the same manner. Certain values of pH, H_2O/Si molar ratio as well as aging time were chosen. The combined mixtures were stirred approximately for 15 min and then subjected to the electrospinning process in the certain periods from the catalyst addition until the solution gelled.

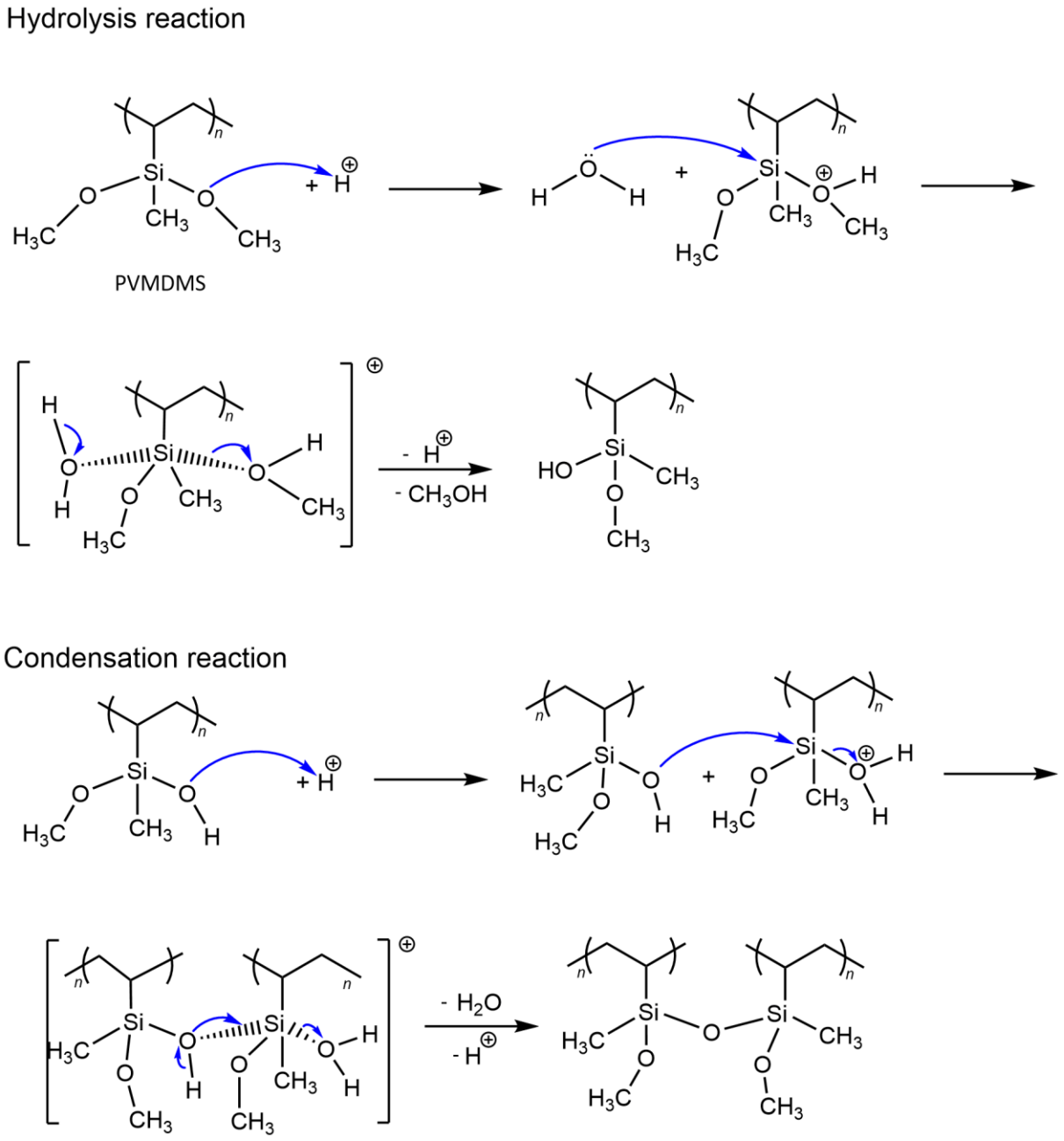

Figure 14: Schematic representation of PVMDMS sol-gel processing under acidic conditions, including hydrolysis and condensation reaction respectively, and the resulting Si-O-Si bridges between polymer chains. The reactions were remade based on the literature. [26]

Table 5: Prepared samples of PVMDMS in acidic MeOH solution for the gelation time determination in sol-gel processing.

Polymer PVMDMS	[wt.%]	**H_2O/Si** [mol/mol]	**pH**	**Polymer PVMDMS**	[wt.%]	**H_2O/Si** [mol/mol]	**pH**
KSH1-48	12	0.81	1	KSH3-48	24	1.06	5
KSH1-48	12	0.81	2	KSH3-48	24	1.06	6
KSH1-48	12	0.81	3	KSH5-48	12	0.81	1
KSH1-48	12	0.81	4	KSH5-48	12	0.81	2
KSH1-48	12	1.87	1	KSH5-48	12	0.81	3
KSH1-48	12	2.50	2	KSH5-48	12	0.81	4
KSH1-48	12	2.57	3	KSH5-48	12	0.81	5
KSH1-48	12	2.44	4	KSH5-48	12	0.81	6
KSH1-48	12	2.44	5	KSH5-48	12	1.87	1
KSH1-48	12	2.44	6	KSH5-48	12	2.50	2
KSH1-48	12	4.89	1	KSH5-48	12	2.57	3
KSH1-48	12	4.89	2	KSH5-48	12	2.44	4
KSH1-48	12	4.89	3	KSH5-48	12	2.44	5
KSH1-48	25	0.77	1	KSH5-48	12	2.44	6
KSH1-48	25	1.02	2	KSH5-48	12	4.89	1
KSH1-48	25	1.05	3	KSH5-48	12	4.89	2
KSH1-48	25	1.00	4	KSH5-48	12	4.89	3
KSH1-48	25	1.00	5	KSH5-48	24	0.81	1
KSH1-48	25	1.00	6	KSH5-48	24	1.08	2
KSH1-48	36	0.45	1	KSH5-48	24	1.11	3
KSH1-48	36	0.61	2	KSH5-48	24	1.06	4
KSH1-48	36	0.62	3	KSH5-48	24	1.06	5
KSH1-48	36	0.59	4	KSH5-48	24	1.06	6
KSH1-48	36	0.59	5	KSH10-48	12	0.81	1
KSH1-48	36	0.59	6	KSH10-48	12	0.81	2
KSH3-48	12	0.81	1	KSH10-48	12	0.81	3
KSH3-48	12	0.81	2	KSH10-48	12	0.81	4
KSH3-48	12	0.81	3	KSH10-48	12	0.81	5
KSH3-48	12	0.81	4	KSH10-48	12	0.81	6
KSH3-48	12	1.87	1	KSH10-48	12	1.87	1
KSH3-48	12	2.50	2	KSH10-48	12	2.50	2
KSH3-48	12	2.57	3	KSH10-48	12	2.57	3
KSH3-48	12	2.44	4	KSH10-48	12	2.44	4
KSH3-48	12	2.44	5	KSH10-48	12	2.44	5
KSH3-48	12	2.44	6	KSH10-48	12	2.44	6
KSH3-48	12	4.89	1	KSH10-48	12	4.89	1
KSH3-48	12	4.89	2	KSH10-48	12	4.89	2
KSH3-48	12	4.89	3	KSH10-48	12	4.89	3
KSH3-48	24	0.81	1	KSH30-18	10	1.00	1
KSH3-48	24	1.08	2	KSH30-18	10	1.00	2
KSH3-48	24	1.11	3	KSH30-18	10	1.00	3
KSH3-48	24	1.06	4	KSH30-18	10	1.00	4

Polymer PVMDMS		H_2O/Si	pH	Polymer PVMDMS		H_2O/Si	pH
	[wt.%]	[mol/mol]			[wt.%]	[mol/mol]	
KSH30-18	10	1.00	5	KSH30-18	30	0.82	3
KSH30-18	10	1.00	6	KSH30-18	30	0.78	4
KSH30-18	10	2.66	1	KSH30-18	30	0.78	5
KSH30-18	10	3.07	2	KSH30-18	30	0.78	6
KSH30-18	10	3.15	3	KSH30-18	30	0.40	4
KSH30-18	10	3.00	4	KSH30-18	30	0.78	5
KSH30-18	10	3.00	5	KSH30-18	30	0.81	6
KSH30-18	10	3.00	6	KSH30-18	40	0.44	1
KSH30-18	10	1.52	4	KSH30-18	40	0.62	2
KSH30-18	10	3.00	5	KSH30-18	40	0.64	3
KSH30-18	10	3.14	6	KSH30-18	40	0.25	4
KSH30-18	10	6.00	1	KSH30-18	40	0.50	5
KSH30-18	10	6.00	2	KSH30-18	40	0.52	6
KSH30-18	10	6.00	3	KSH30-18	40	0.50	4
KSH30-18	20	1.18	1	KSH30-18	40	0.50	5
KSH30-18	20	1.66	2	KSH30-18	40	0.50	6
KSH30-18	20	1.40	3	KSH30-18	50	0.30	1
KSH30-18	20	0.68	4	KSH30-18	50	0.41	2
KSH30-18	20	1.33	5	KSH30-18	50	0.43	3
KSH30-18	20	1.40	6	KSH30-18	50	0.33	4
KSH30-18	20	1.33	4	KSH30-18	50	0.33	5
KSH30-18	20	1.33	5	KSH30-18	50	0.33	6
KSH30-18	20	1.33	6	KSH30-18	50	0.17	4
KSH30-18	30	0.69	1	KSH30-18	50	0.33	5
KSH30-18	30	0.97	2	KSH30-18	50	0.35	6

4.7 Preparation of carrier-polymer mixtures

PVP was weighted and added into the PVMDMS solution with specific mass fractions ranging from 0.2 to 5.0 wt.% PVP. PVP was also dissolved in dry methanol in order to make blank samples without PVMDMS. Mixtures of PVMDMS and PVP in MeOH and blank PVP samples used for electrospinning process are given in Table 6. The mixture was stirred in a plastic container at ambient conditions until the solution was transparent.

Table 6: Representation of polymer solution mixtures of PVMDMS and PVP in MeOH (left) as well as blank PVP mixtures in MeOH (right) for electrospinning.

Polymer PVMDMS	[wt.%]	**PVP** [wt.%]	**PVP** [wt.%]
KSH1-48	10	0.2	0.2
KSH1-48	10	2.0	1.0
KSH1-48	10	5.0	2.0
KSH1-48	50	0.2	4.0
KSH1-48	50	2.0	6.0
KSH1-48	50	5.0	8.0
KSH30-18	10	0.2	10.0
KSH30-18	10	2.0	15.0
KSH30-18	10	5.0	
KSH30-18	50	0.2	
KSH30-18	50	2.0	
KSH30-18	50	5.0	

4.8 Electrospinning process

The polymer solution was placed in a syringe with a volume of 1 mL connected with the pump which was used to supply a steady flow. The feed rate was set to 0.5 mL/hr. The used needle was a blunt type of diameter 21G and dimensions 0.80 × 22 mm. The voltage was varied between 0–40 kV and was set to the value that the electrospinning appeared stable, assessed by the presence of Taylor cone. The electrospun fibers were collected on the collector at 15 cm fixed distance. The collector was covered by aluminum foil. All the experiments were carried out at ambient conditions. Table 7 shows prepared samples of PVMDMS in MeOH for electrospinning. Samples including sol-gel processing (see Chapter 4.6) and carrier-polymer mixtures (Chapter 4.7) were electrospun in the same manner.

Table 7: Used solutions of PVMDMS in MeOH for elecrospinning.

Polymer PVMDMS	[wt.%]	**Polymer PVMDMS**	[wt.%]	**Polymer PVMDMS**	[wt.%]
KSH1-48	100	KSH12.5-48	20	KSH20-48	20
KSH2-48	100	KSH12.5-48	25	KSH30-18	10
KSH10-48	60	KSH12.5-48	30	KSH30-18	20
KSH10-48	40	KSH12.5-48	60	KSH30-18	30
KSH12.5-48	5	KSH15-72	5	KSH30-18	60
KSH12.5-48	10	KSH15-72	10	KSH30-18	70
KSH12.5-48	15	KSH15-72	40	KSH30-18	80

5 RESULTS AND DISCUSSION

5.1 Characterization of PVMDMS

PVMDMS was synthetized from VMDMS using DTBP as initiator. The concentration of DTBP was varied in order to prepare polymers of different M_n. Characterization of the obtained PVMDMS was performed by FT-IR spectroscopy in order to study disappearance of characteristic functional group signals of the monomer. NMR analysis was employed with the aim to determine M_n of thus prepared polymers. DLS measurements were carried out in order to confirm the calculated M_n with respect to data obtained from NMR investigation.

5.1.1 Polymer structure

PVMDMS was analyzed by FT-IR spectroscopy in order to evaluate polymer products of various DTBP ratios employed during FRP in terms of disappearance of characteristic functional groups vibration signals after FRP visible via FT-IR spectroscopy. Depending on the initiator concentration and reaction time, different molecular weights are expected. Experimental FT-IR spectroscopy data were compared to the simulated vibrational frequencies of the PVMDMS model molecule. The spectrum of the monomer VMDMS was recorded for comparison. The initiator DTBP was subjected to the FT-IR analysis for completeness. It is assumed that the initiator is completely decomposed after the polymerization reaction and hence does not show any significant peaks in the spectra. The spectra of VMDMS, PVMDMS and DTBP are shown in Figure 15. Moreover, the most important peaks are summarized in the Table 8.

The FT-IR spectrum of the monomer VMDMS shows peaks assigned to the vinyl group in the range 3 000–1 000 cm^{-1} and most of them either disappeared or changed the peak shape compared to PVMDMS. Zu et al. reported C-H bands in the region 3 000–1 000 cm^{-1} as signals of methyl groups and/or the aliphatic hydrocarbon chains of the PVMDMS. [46]

The very weak peak at 3 057 cm^{-1} is attributed to C-H stretching vibrations of vinyl group and disappeared in the PVMDMS spectrum in comparison to the monomer VMDMS. The weak and moderate bands at 2 941 and 2 837 cm^{-1} are assigned to C-H stretching of the vinyl and methyl group. While the weak peak at 1 597 cm^{-1} is assigned to the C=C stretching and disappeared in the PVMDMS again indicating successful polymerization reaction. [46–48]

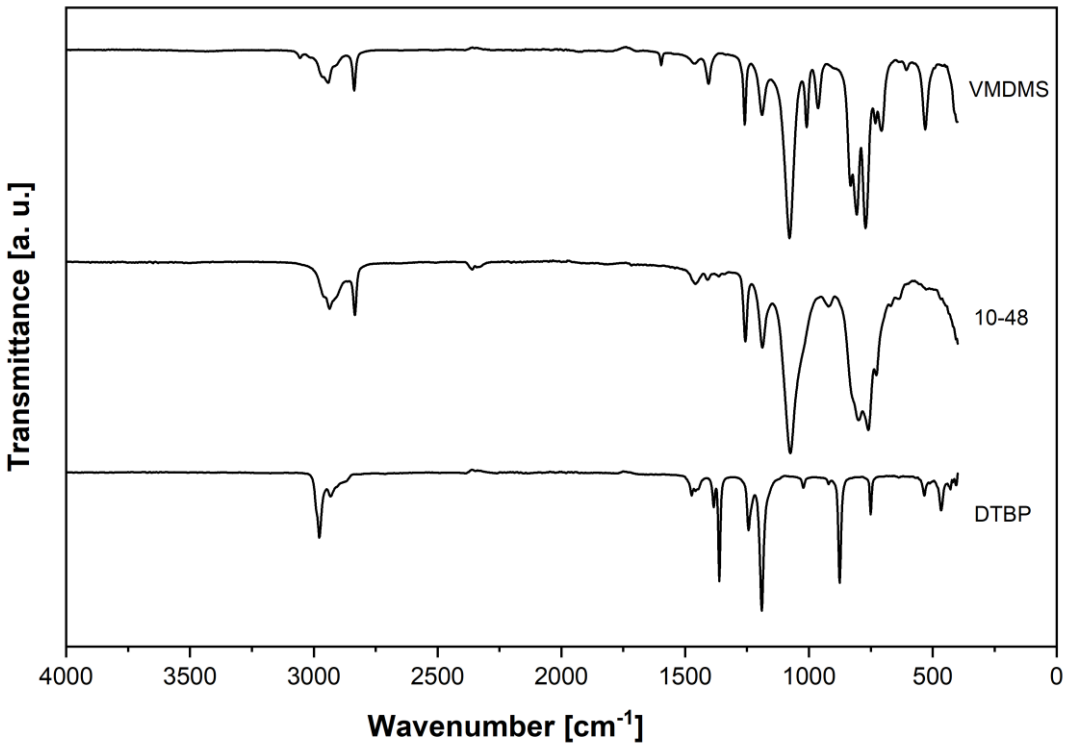

Figure 15: FT-IR spectra of VMDMS, PVMDMS KSH10-48 and DTBP.

The bands located at 1 404 $cm^{-1}$and 1 461 cm^{-1} correspond to the symmetric deformation and bending vibrations of C-H bonds overlapped with $=CH_2$ scissoring vibrations. Alkane bending of the polymeric carbon backbone was assigned to 1 363 cm^{-1} and appeared in all the polymeric products. Furthermore, the signal at 1 009 cm^{-1} corresponds to CH_2 rocking vibrations of the vinyl group and was observed only in VMDMS. [46, 48]

The strong peaks at 1 078 cm^{-1} for VMDMS and ~1 076 cm^{-1} for prepolymerized samples are related to the Si-O stretching vibration. These signals remain the same for monomer and polymer because the Si-O bond is not affected by the polymerization reaction.

The signal at 964 cm^{-1} is related to CH_2 or CH wagging vibrations. [49] The moderate band between 800–760 cm^{-1} appeared in the PVMDMS is assigned to the CH_2 rocking vibration, CH_2 twisting, stretching and asymmetric stretching of Si-C bond. These peaks indicate the methyl-rich structure of PVMDMS. [47]

The medium peak at 530 cm^{-1} is assigned to the C-H bending of vinyl group and this signal disappeared in the PVMDMS. [47] [46]

Interestingly, there is no significant peak at 3 500 cm^{-1} which is attributed to the –OH group. Therefore, it may be concluded that the methoxygroups of PVMDMS have not reacted by hydrolysis reaction. In addition, polysiloxane moieties which would be expected from hydrolysis and condensation reactions of the methoxysilyl groups of PVMDMS and are

Table 8: Observed vibrational frequencies (cm^{-1}) of VMDMS and PVMDMS, experimental and simulated data. Abbreviations: s, strong; m, medium; w, weak; v, very; b, broad; sh, shoulder; ν, stretching; δ, deformation; ω, wagging; π, twisting; γ, rocking; σ, scissoring; β, bending; subscript s, symmetrical and a, antisymmetrical.

Experimental								**Simulation**		
VMDMS		**1-48**	**10-48**	**20-48**	**30-18**		**Vibrational assignment**	**PVMDMS**		**Vibrational assignment**
3 057	vw						ν_a(C-H), vinyl	3 048	w	$\nu_a(CH_2)$
2 941	m b	2 936	2 936	2 936	2 936	m b	ν(C-H), vinyl and methyl	3 019	m	$\nu_a(CH_2)$
2 837	m	2 834	2 834	2 834	2 834	m	ν(C=C), $\nu_s(CH_3)$	3 007	m	$\nu_a(CH_2)$
			2 360	2 361	2 360	vw	ν(C=O), CO_2	2 985	m	$\nu_a(CH_2)$
			2 341			m sh	ν(C=O), CO_2	2 929	m	$\nu_s(CH_2)$
1 597	w						ν(C=C)	1 454	w	$\sigma(CH_2)$
1 461	vw	1 457	1 458	1 458	1 458	vw	δ_s(C-H), $\sigma(=CH_2)$	1 412	vw	$\sigma(CH_2)$
1 406	m	1 410	1 410	1 409	1 409	vw	δ_s(C-H), $\sigma(=CH_2)$	1 319	vw	β(CH), vinyl
			1 363	1 364	1 363		β(CH), alkane	1 241	w	$\sigma(CH_3)$; β(CH), vinyl
1 259	m	1 257	1 257	1 257	1 257	m	β(CH), vinyl	1 166	m	ν_a(Si-O), $\gamma(CH_3)$
1 190	m	1 188	1 188	1 188	1 189	m	ν(Si-O), ν(C-C)	1 076	s	ν_s(C-O), ν_a(Si-O), ν_a(C-C), $\pi(CH_2)$
1 078	s	1 075	1 075	1 076	1 077	s	ν(Si-O), $\gamma(CH_3)$	922	vw	ν_s(C-C), γ(CH)
1 009	m						$\gamma(CH_2)$, vinyl	905	vw	ν(C-C), vinyl; $\gamma(CH_3)$
963	m	917	920	920	920	vw	ω(CH)	852	vw	$\gamma(CH_3)$; ω(C-C), vinyl
832	m sh						ν(Si-C), ν(C-C), $\gamma(CH_2)$, $\pi(CH_2)$	814	m	ν_s(Si-O), $\gamma(CH_3)$, γ(Si-O), γ(Si-C), $\gamma(CH_2)$, vinyl
806	s	800	799	800	801	s sh	ν(Si-C), $\gamma(CH_2)$, $\pi(CH_2)$	795	m	ν_s(Si-C), ν_s(Si-O), $\gamma(CH_2)$, $\omega(CH_3)$
771	s	760	760	762	762	s	ν(Si-C), $\gamma(CH_2)$, $\pi(CH_2)$	755	w	ν_s(Si-C), ν_a(Si-O), $\gamma(CH_2)$, $\omega(CH_3)$
732	m sh	728	728	729	729	m sh	ν(Si-C), $\gamma(CH_2)$, $\pi(CH_2)$	713	w	ν_a(Si-O), $\omega(CH_3)$
707	m sh						ν(Si-C), $\gamma(CH_2)$, $\pi(CH_2)$	677	vw	ν_a(Si-O), ν_a(Si-C), γ(CH)
607	vw						ν(Si-C), $\gamma(CH_2)$, $\pi(CH_2)$	632	vw	ν_s(Si-O), ν_a(Si-C), $\gamma(CH_2)$
530	m						β(CH), vinyl	521	vw	ν_a(Si-C), $\sigma(CH_2)$, vinyl; $\gamma(CH_3)$, σ(Si-O), ω(Si-C)
								490	vw	β(CH), vinyl; β(Si-O), β(Si-C)

typically indicated by signals at ~1085 cm^{-1} and ~780 cm^{-1} according to the literature can neither be found in the monomer nor the polymerized VMDMS. [46] [49]

In order to confirm the FT-IR spectroscopic signals of PVMDMS, a model molecule of the polymer containing 5 monomer units was calculated (see structure in Figure 16). Table 8 shows the most intense signals in the simulated spectrum and attributed vibrations. The simulated spectrum based on the calculated PVMDMS model is shown in Figure 17 in comparison to the experimental spectrum. The simulation exhibits a good agreement with the experimental data. Peak splitting and shoulder peaks revealed in the experimental data due to overlapping of FT-IR signals.

To conclude, the results of the FT-IR analysis confirmed the polymerization of the vinyl groups of VMDMS to yield a polyvinylsilane. The methoxy groups of PVMDMS remain stable after polymerization and are available for postpolymerization reactions.

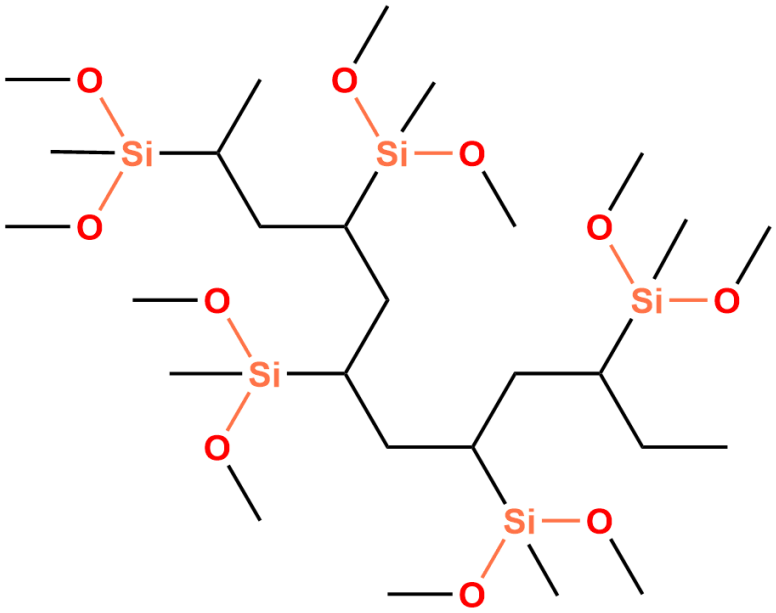

Figure 16: Simulated PVMDMS molecules used for prediction of vibrational frequencies.

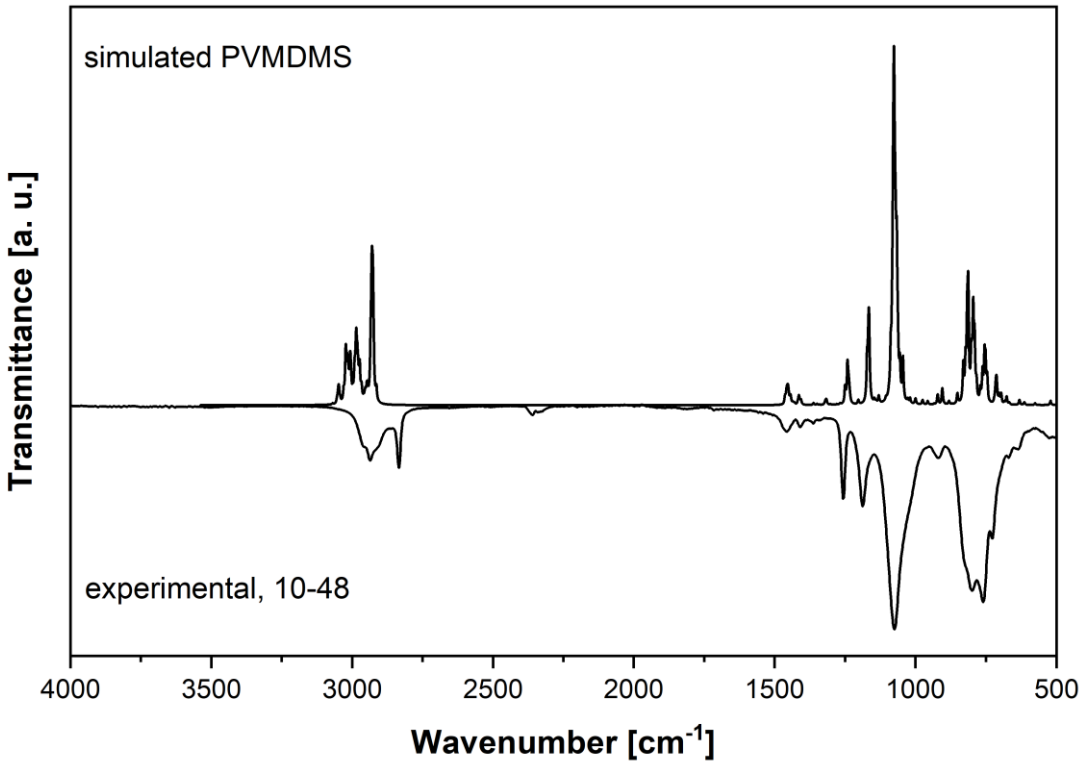

Figure 17: Simulated and experimental IR spectra of PVMDMS.

5.1.2 Molecular weight

Polymerization reactions of VMDMS were carried out with various molar ratios of DTBP/VMDMS in order to change concentration of radical starter to promote FRP. Hence, the molecular weight was only sought upon change of radical starter concentration in this work. Polymers of viscous liquid, gel and soft solid texture are obtained. In order to determine the M_n of PVMDMS, the NMR end-group analysis was performed. The highest M_n was determined for KSH1-48 and KSH30-18, with 53 and 41 kg/mol, respectively. KSH5-48 exhibited M_n of 10 kg/mol and KSH10-48 of 25 kg/mol. Determination of M_n for KSH1-48 was repeated with another PVMDMS batch to verify the PVMMS after FRP. Table 9 shows an overview of degree of polymerization (DP) and resulted M_n of synthetized PVMDMS in comparison to Kanamori et al. FRP syntheses of PVMDMS. [3]

Kanamori et al. reported data about FRP of VMDMS including polymerization time, molecular weight, degree of polymerization, polydispersity and conversion. The Kanamori results showed DP of 22 for 1 mol.% of initiator employed. While conversion slightly increased from 91 to 99 % with extension of polymerization duration from 24 to 72 hr, polydispersity index (PDI) increased from 1.86 to 2.09 compared to 24 and 72 hr polymerization duration. An increase of the amount of radical starter to 5 mol.% resulted in even higher DP and M_n. DP increased to 27 and PDI reached values of 2.57, the conversion was reported as 99 %.

Table 9: Experimental data of DP and resulted M_n for PVMDMS for four different concentrations of the initiator obtained from NMR and Kanamori et al. data of PVMDMS for comparison obtained by SEC. [46]

Experimental PVMDMS			**Kanamori et al.**		
Initiator [mol. %]	**DP**	M_n [g/mol]	**DTBP** [mol.%]	**DP**	M_n [g/mol]
1	400	52 991	1	22	2 880
5	77	10 308	5	26	3 501
10	187	24 820			
30	306	40 543			

The NMR end-group analysis as performed on the synthetized PVMDMS in this thesis, showed very different results in comparison to Kanamori et al., even though the same polymerization conditions were employed. Generally, FRP with use of DTBP as a radical starter results two distinct chain end-groups, either *tert*-butoxy or methyl. Hovewer, the signal of *tert*-butoxy was the only one used for the calculation of M_n based on the recorded NMR signal. The representative NMR ^{1}H-^{13}C spectrum of PVMDMS based M_n determination is depicted in Figure 18. Since methyl groups could not be detected as a chain end-group, these moities were neglected. It is, however, very clear that for a more precise evaluation, the ratio between *tert*-butoxy as well as methyl chain end-group has to be taken into account. Therefore, in a case of more chain end-groups than one, all the chain end-groups have to be used for calculation. Otherwise the signal of polymeric chain is associated only to one end-groups but might then reveal in a higher value of M_n. Thus, the experimentally evaluated M_n for the synthetized PVMDMS could not be determined on an absolute scale via the applied chain end-group NMR analysis. End-groups can be various nature compared to the basic model of DTBP decomposition. There might be undefined end-groups which arise from the chain transfer reactions due to formation of additional radicals in this step and proceeding in the chaing growth. [50] Generally, the M_n in an mathematical average of chain length therefore shows how many molecules are shorter or larger than the determined M_n. However, the literature reports that the end-group analysis becomes insensitive above 25 kg/mol due to the low concentration of end-groups present in the sample. [51] The number-average molecular weight represents the number of units within a polymeric chain and neglects the PDI which might also be of high relevance. Due to the difficulties of dissolving the synthetized PVMDMS with initiator concentration above 11 mol.% in a suitable solvent for SEC analysis, SEC has not been employed however it can reveal more precise evaluation of M_n as well as M_w. An advantage of SEC analysis, which Kanamori et al. used, is an acquiring of PDI and therefore cover the broadness of molecular weight represented by various chain length in the polymerization product.

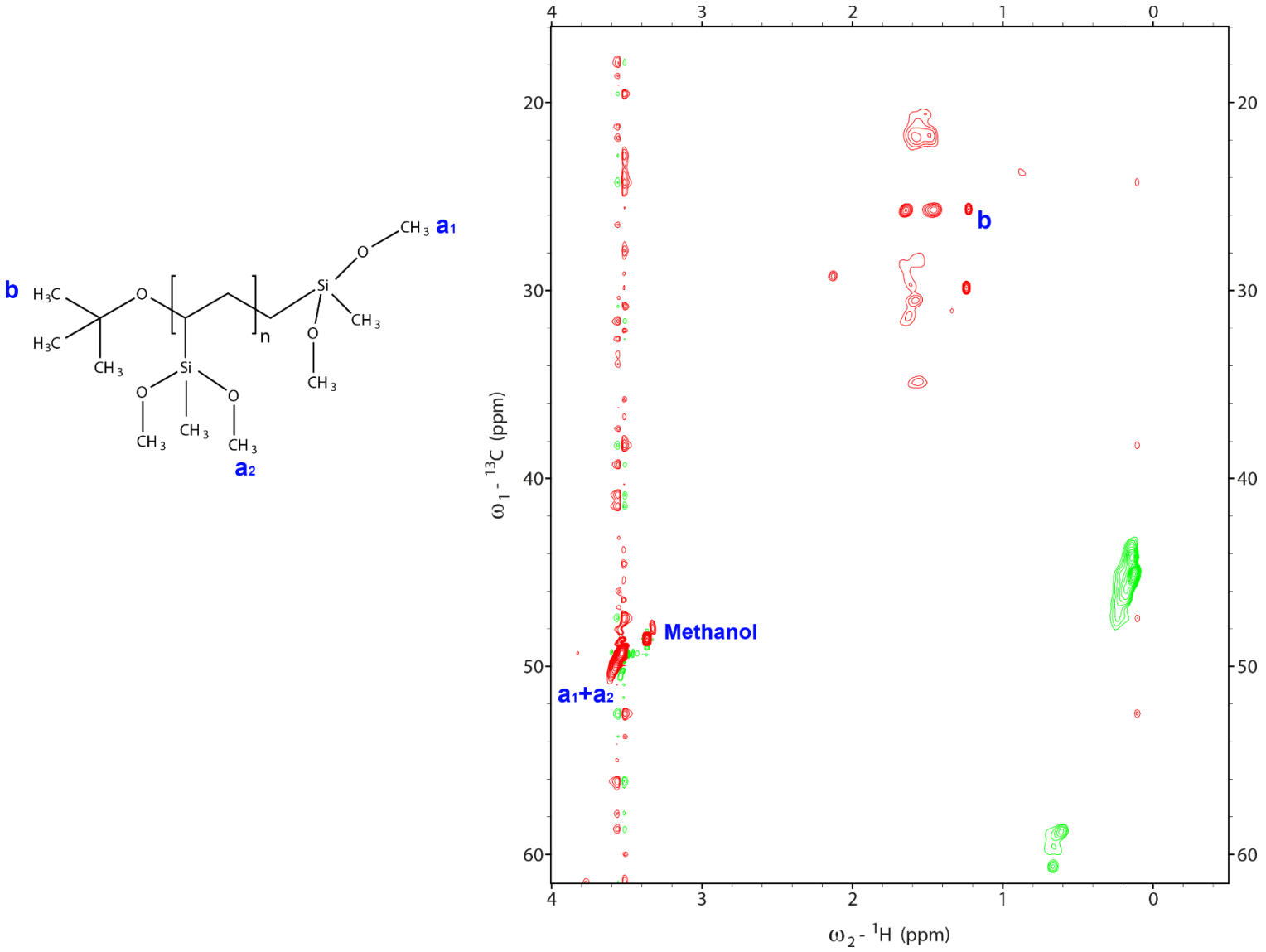

Figure 18: ^{1}H-^{13}C NMR spectrum for KSH5-48 and the structure of the molecule with highlighted atoms for calculation.

Polymerizations with very low or on the other hand very high amounts of DTBP resulted in very high M_n of PVMDMS and the dependence of M_n upon DTBP concentration is depicted in Figure 19.

From literature it is known that if the concentration of initiator in FRP is low, the initiator in the reaction is quickly consumed and therefore not accessible for the termination reaction. Therefore, termination typically does not occur via reaction with the initiator but with higher probability by chain combination. Disproportionation reaction would not be in favor in the bulk polymerization due to the increasing viscosity of the reaction mixture

On the contrary, if the concentration of the initiator is high, many molecules are activated from the beginning of FRP. Therefore the chance for combination of two activated polymeric chain is even higher. The concentration of the initiator is very high and the probability to meet activated monomer and polymer or two polymeric chains is in favor. This might often result in termination reactions and in higher PDIs. [52] [14]

The reaction mixture contains a huge amount of reactive species such as activated polymer chains, radicals and activated monomers. Consequently, another termination can occur by activated chain transfer either to monomer, initiator, or polymer in the case of bulk polymerization. And thereby, the chain transfer can contribute to the termination process of the growing chain as well. In the chain transfer, the new radical species is always formed. According to reported data in the literature, vinyl polymerization is sensitive to the transfer reactions. Batch polymerization of vinyl leads to termination predominantly by transfer.

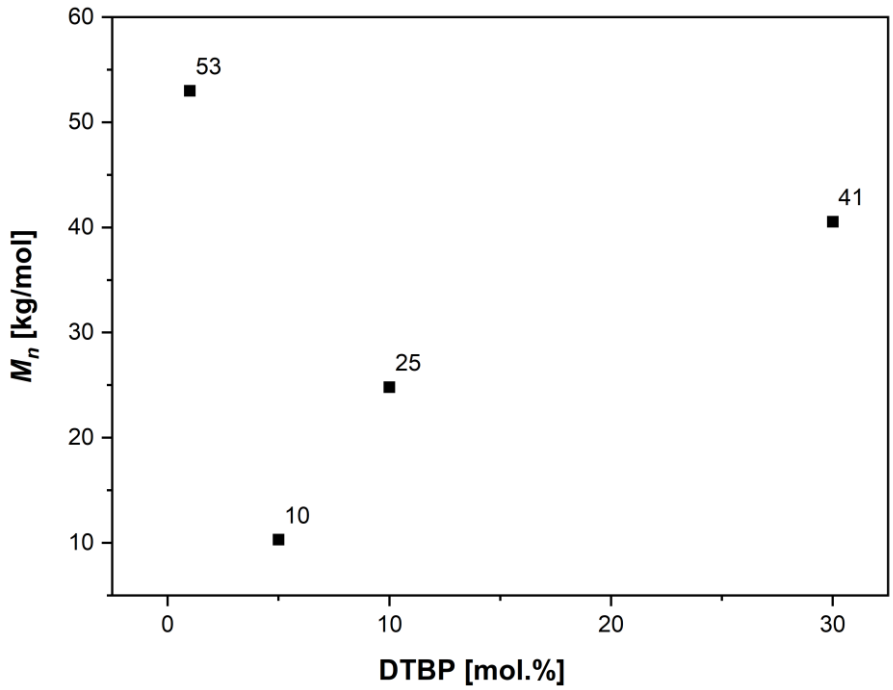

Figure 19: Number-average molecular weight dependence on concentration of radical starter DTBP used in the synthesis of PVMDMS.

The reaction is also characteristic for branching due to termination reaction by combination of polymeric chains. The reaction mixture consists of various lengths of the polymer and therefore upon polymeric chain combination, the molecular weight of the resulting polymer depends on both chains combined in the termination step. [53] [54]

Chain transfer of monomer to initiator begins by hydrogen subtraction from a monomer molecule and thus the monomer is activated. The subtracted hydrogen is transferred to the polymeric chain and terminates the growth of the chain. Created activated monomer do not tend to proceed further reaction. [52]

The transfer to initiator is another type of the chain transfer and allows further propagation reaction. It is a special type because only in this case, the termination of the chain growth occurs and another chain can be activated by the new resulted radical as well. The initiator chain transfer to a polymeric chain terminates the polymeric chain growth and forms initiator radical. Consequently, the initiator radical can proceed reaction by activation of monomer and the chain growth and further propagation can begin. Peroxides, such as DTBP are sensitive to this type of chain transfer. Scorah el al. reported production of highly branched vinyl functionalized polymer in the presence of peroxide as an initiator in a bulk polymerization. Thus prepared polymers revealed in insoluble gels very early in the polymerization. To conclude, nature of the vinyl tends to undergo transfer reactions during polymerization and it has an impact on the chain structure and resulting physical properties. [52] [55]

The last possibility for chain transfer is a transfer to polymer. The process is initiated by a polymeric chain hydrogen abstraction by an activated polymeric chain. Termination of the chain growth occurs on the hydrogen receiving chain. The other chain becomes activated, either on the end or also on the chain backbone which might reveal in a branched polymer. As a result, the number of polymerized monomer unit is not changing because this reaction takes place between polymer chains already created by FRP. Degree of polymerization is therefore not affected because new monomer units are not engaged in this chain growth. [52]

The overall result of the chain transfer is a decrease of the polymeric chain lengh because the chain growth is affected. Very short polymers can be formed in a case that the chain transfer rate is faster compared to the propagation reaction. Above mentioned types of chain transfer could affected the FRP of VMDMS with regards to DTBP concentration presented in the reaction mixture. FRP is characteristic for the growth mechanism on the active site of the polymer chain. Number of these active sites varies upon concentration of radical presented in the reaction mixture. Very high concentration of radical starter will activate more monomer molecules in the mixture.

E.g. transfer to initiator might reveal in very broad PDI and therefore properties of PVMDMS might be affected. Transfer to chain might reveal in branched polymer which might

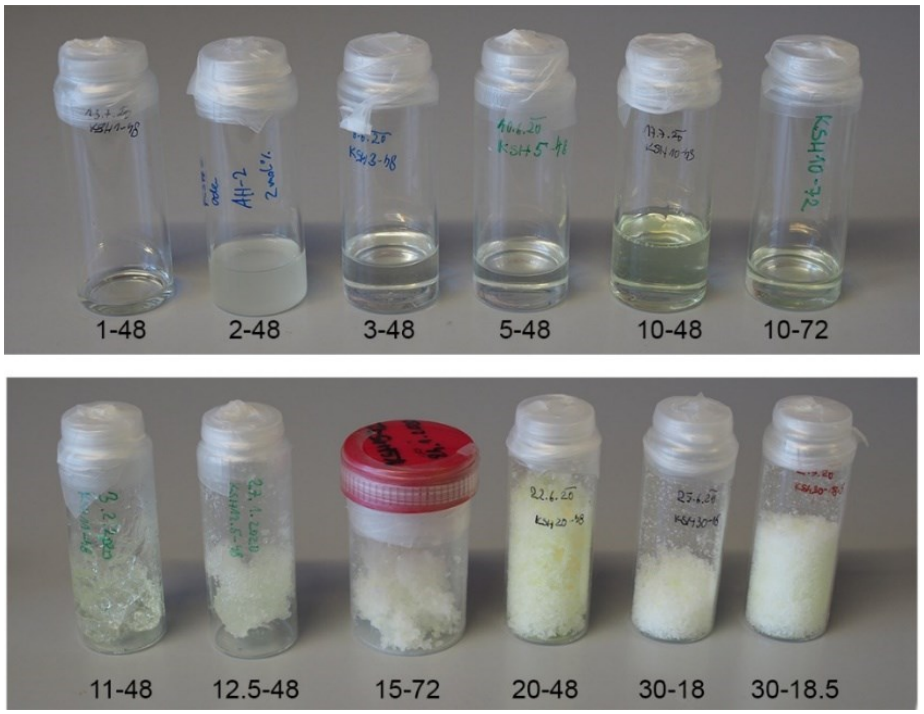

Figure 20: PVMDMS products. Upper row shows viscous polymers and down row gels and soft solids. The first number stands for molar percentage of the initiator DTBP and the second for duration of polymerization.

influence texture and solubility of the polymer significantly. Very large chains can contribute to the solid-like texture of the polymer but still the analyzed M_n can be similar to lower DTBP employed in the FRP as might be assumed from the NMR end-group analysis of sample 1 and 30 mol.%. PVMDMS in a range of initiator 1 to 10 mol.% resulted in viscous liquid product and concentration higher, 11–30 mol.% resulted in jelly and soft solid polymeric products. To conclude, the polymer appearance was changing from liquid via gel to solid upon increase in the radical starter concentration. Representation of samples of various textures are given in Figure 20.

5.1.3 Size evaluation

In order to confirm the M_n data from NMR spectroscopy, polymer size distribution analysis by DLS was performed. Parameter z-average was analyzed via DLS which probes hydrodynamic mobility either of particle or coil-like polymer in a solution. Basically, the z-average is intensity-based calculated value from a light scattering in a solution upon Brownian motion of suspended particles. [56]

The NMR analysis showed that there is not a linear dependence for the investigated DTBP concentrations. This fact was also confirmed by DLS measurements. DLS data showed that the highest z-average measures appeared in the polymer with 1 mol.% and then above 10 mol.% DTBP. However, samples with DTBP concentration of 15 mol.% results in the

highest z-average, but more than on size signals is obtained and reliability of the measurement is questionable. Overall, samples above 11 mol.% of DTBP showed more sizes during the polymer size distribution analysis probably due to the high PDI of sample. Difficulties in the measurement PVMDMS of higher initiator concentration than 12 mol.% were encountered by DLS.

Experimental z-average of PVMDMS in MeOH in dependence on DTBP concentration is depicted in Figure 21. Data show very distinct increase of z-average when employed 1 or more than 11 mol.% of DTBP. The range of DTBP concentration between 2 to 10 mol.% seems to have a linear trend of z-average upon DTBP concentration employed during FRP. Polymers of radical starter concentration ranging from 2 to 11 mol.% revealed in a very strong linear dependence on the radical starter concentration employed during the polymerization synthesis. Overall, the experimental data of DLS analyses showed a good correlation between the z-average radius of gyration representing a size of PVMDMS coil in a solution according and the M_n achieved by NMR. Figure 22 shows the linear dependence of z-average of PVMDMS in MeOH upon employed DTBP initiator concentration of 2–11 mol.% during the polymer synthesis. Certain range of used radical starter concentration in FRP can result in a gradually increasing M_n. Due to higher concentration of present radicals, more active chains can be introduced at the same time. As the number of active site increases, the degree of polymerization changes but the kinetics of the reaction is not influenced. [51]

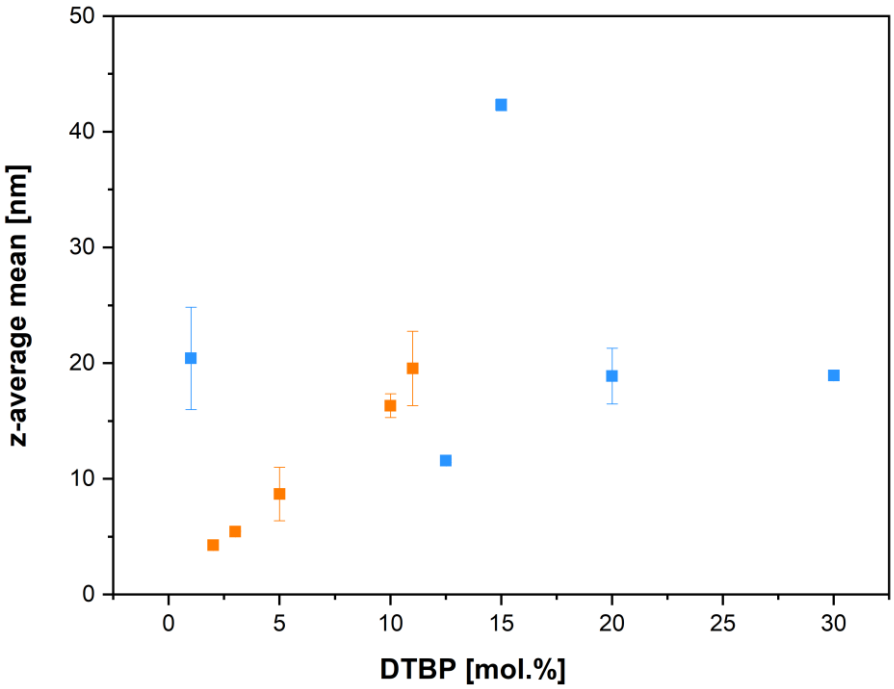

Figure 21: Z-average dependence on concentration of the radical starter DTBP for the synthetized PVMDMS.

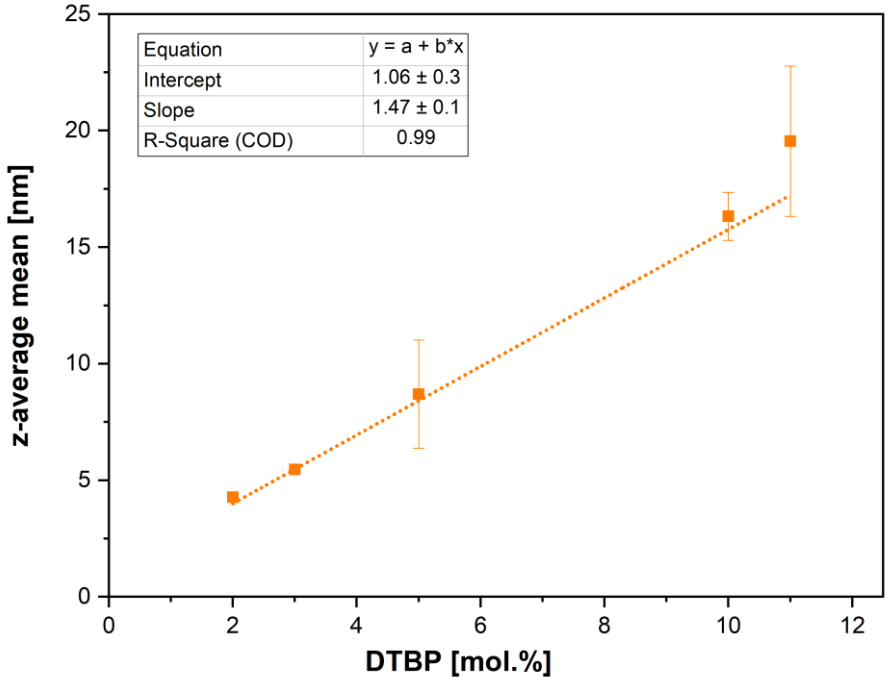

Figure 22: Z-average linear dependence of certain synthetized PVMDMS in regard to concentration of DTBP as a radical starter.

5.2 Electrospinning of PVMDMS

The synthetized PVMDMS of various M_n was subjected to the electrospinning process with the aim to produce fibers. Solutions of PVMDMS in MeOH in various concentrations have been tested. Specifically, the polymers KSH1-48, KSH2-48, KSH10-48, KSH12.5-48, KSH15-72, KSH20-48, KSH30-18 were examined. Samples differed in M_n of PVMDMS. As a short summary: The samples KSH1-48, KSH2-48, KSH10-48 formed droplets or coating after electrospinning. It is clear that fiber formation can only be based on entanglement of the polymer (silicone) chains, since typically only two-dimensional (2D) interconnectivity is given by the radical polymerization process. Figure 23 shows microscopic images of representative samples of KSH12.5-48 and KSH15-72 in concentrations ranging from 5 to 60 wt% in MeOH. Although very high concentrations of PVMDMS were employed, the system tended to form droplets and coating like structure after the electrospinning process. KSH20-48 showed droplet and coating formation as well. KSH30-18 at concentration ranging between 10 to 30 wt.% resulted in droplet and coating structure after electrospinning. Interestingly, KSH30-18 resulted in few fiber fragments at very high concentration ranging from 60 to 70 wt.% after electrospinning and the diameter was assessed roughly to 10 µm. KSH30-18 exhibited high M_n upon NMR analysis and was solid polymer after FRP. According to the literature about radical starter in FRP and the resulting reaction mechanism, KSH30-18 might be branched polymer in

comparison to KSH1-48. Figure 24 depicts samples KSH30-18 of various concentration employed during the electrospinning process.

For many of the tested precursors, electrospinning resulted in droplet formation (electrospraying) and only upon increase of the molecular weight of PVMDMDS combined with higher concentration, transition in fiber formation (electrospinning) occured. Based on published work, incipient and incomplete fiber formation is observed at one entanglement per chain and stable and complete electrospinning was reported for entanglements of ≥ 2.5 per chain. [39] It is assumed that KSH30-18 showed more entanglements compared to other tested PVMDMS electrospinning solutions because viscosity of the electrospinning solution KSH30-18 significantly increased compared to other PVMDMS solutions. It is assumed that an increase in entanglements arises with increase in PVMDMS content in the solution. Higher content of the polymer in solution is accompanied with an increase in the number of entanglements as well as it was described by Gennes as reptation of polymer chains in the presence of fixed obstacles. [40] Munir et al. reported a strong dependence of fiber formation on entanglements regarding to the molecular weight of the used polymer as well as its concentration in the electrospinning solution. [42]

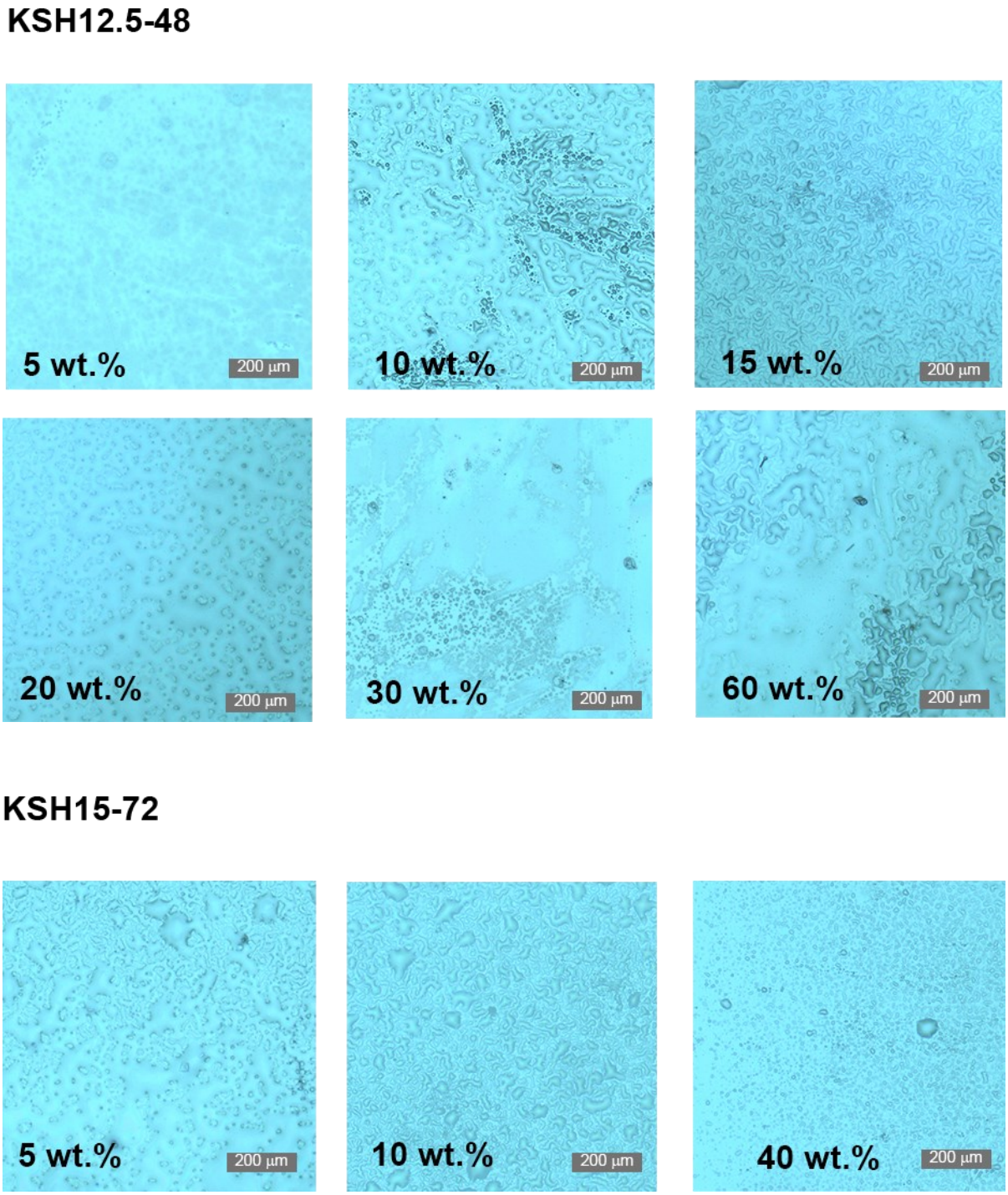

Figure 23: Microscopy images of electrospinning results for KSH12.5-48 and KSH15-72 at various concentration of the PVMDMS in MeOH.

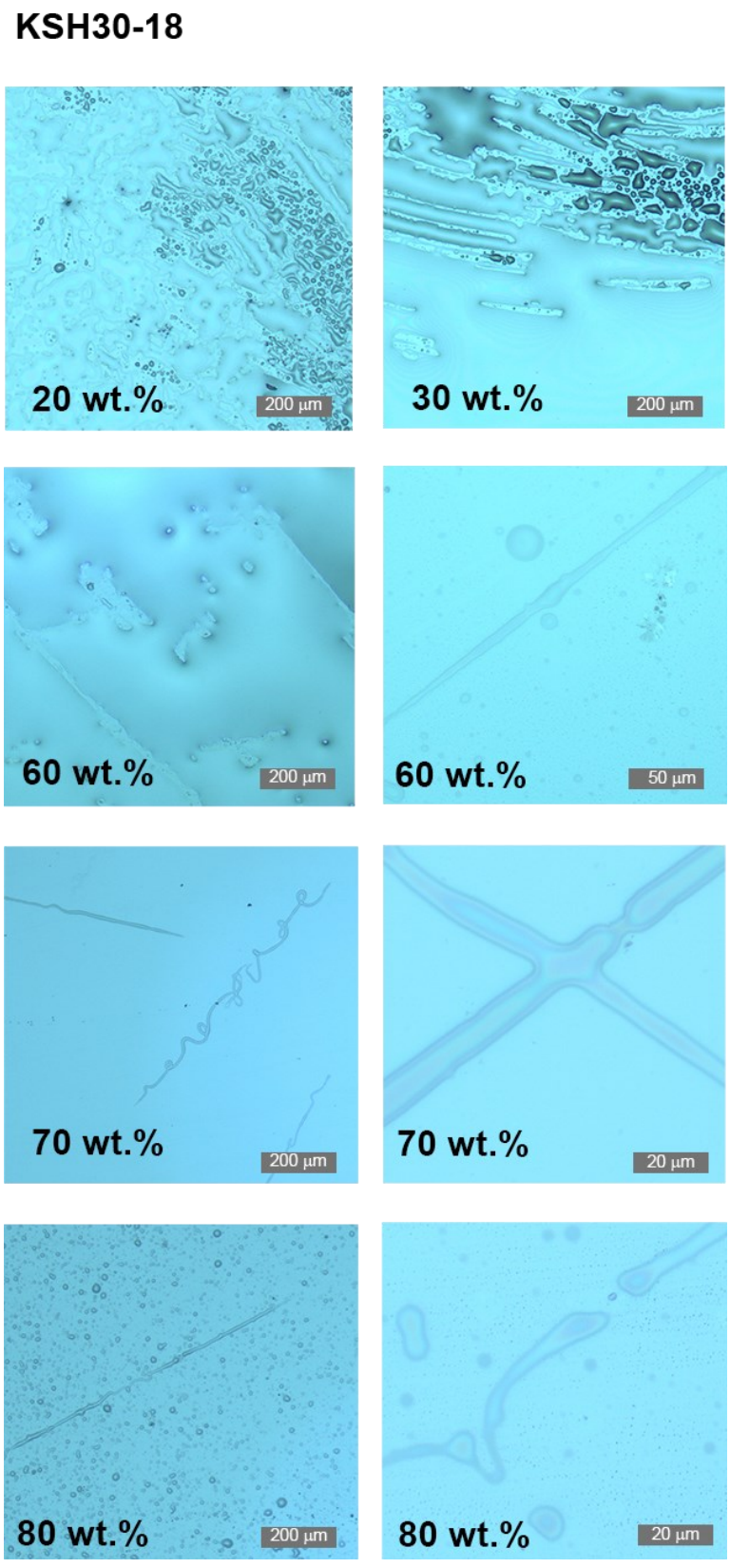

Figure 24: Microscopy images of electrospinning results for KSH30-18 at various concentration in MeOH.

5.3 Carrier-polymer PVMDMS mixtures

Carrier-polymer mixtures are also applied for electrospinning since that produced fibers can bring different properties as well as the spinnability can be enhanced. Electrospinning of PVP is well reported in the literature and the use in this work was primarily due to a good solubility in MeOH compared to another possible carrier-polymers. [42, 43, 57, 58] In this case homogeneous solutions of different polymers are prepared prior to electrospinning and subjected to electrospinning process. Change of the weight fraction of the polymers in the solution can influence the fiber diameter. Interaction between the polymers in a blend plays a significant role in terms of structure, morphology and composition of the prepared fibers. In this thesis, electrospinning experiments with mixtures of PVMDMS and PVP in methanol in various ratios and concentrations were performed out with the purpose of creating a reference system to electrospinning of PVMDMS in methanol. The aim was to investigate fiber formation upon PVMDMS concentration in a blend of carrier polymer and thus conclude differences of fiber structure in regard to electrospinning of PVMDMS in MeOH. As a starting point, pure PVP fibers were prepared according to reference [57].

Figure 25 depicts the evolution of fiber formation from a droplet-like, via a beaded structure into a smooth fiber structure with increasing concentrations of PVP. Concentration of PVP in a range 0.2 to 4 wt.% in MeOH resulted in a droplet formation. Solution of 4 wt.% of PVP showed some jet alignments of small droplets. Therefore, it is assumed that the system proceeds via jet formation but the resulting fibers are not stable or do not arrive dry on the collector and dissolve into droplets. Surface tension of the liquid provide a driving force for droplet formation if the number of entanglements is not sufficient. [39] Solution of 6 wt.% PVP exhibited beads and fiber structures with a fiber diameter of approximately 1 µm. Concentrations of 8 and 10 wt.% PVP resulted in narrow fibers of similar diameter above 1 µm. Solution of 15 wt.% PVP resulted in fiber of approximately 2 µm in diameter. To conclude, the resulting fibers (structure and diameter) are significantly changed as the concentration of the polymer in the solution varies. This is in agreement with published data for PVP electrospinning. [42] Typically the PVP system behaves as other polymers during electrospinning and changes from droplets to fibers. [42] The transition from electrospraying into electrospinning was recognized at the concentration 6 wt.% PVP.

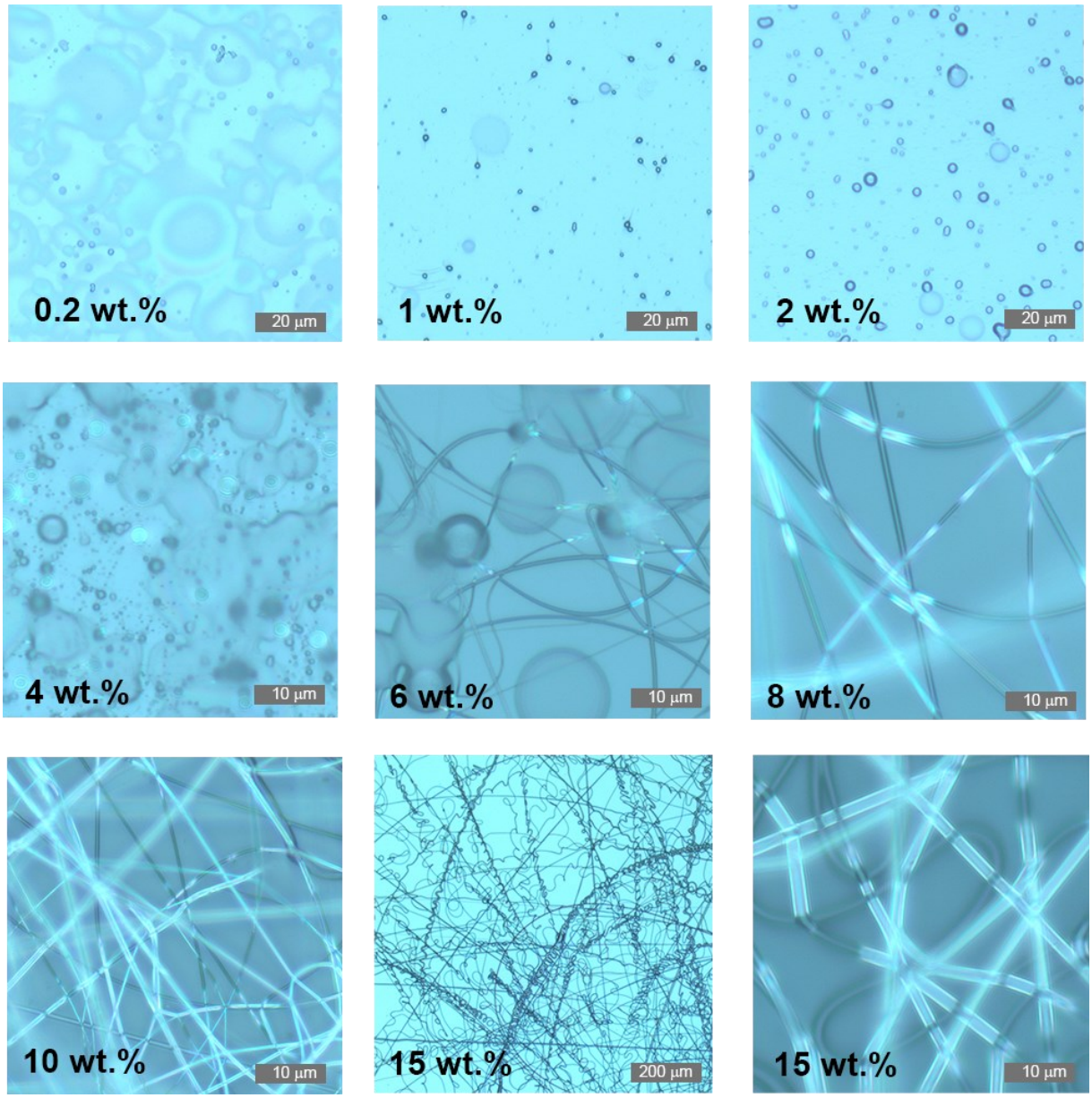

Figure 25: Microscopy images of PVP fibers in MeOH at various concentration of the polymer.

In a second step electrospinning of PVMDMS and PVP blends were tested with mixtures of the prepolymerized PVMDMS and PVP. Preceding experiments of PVP in MeOH revealed fiber formation at 6 wt.% of the polymer and thus, concentration slightly below was chosen in order to keep PVP concentration low and therefore focus on fiber structure influence by PVMDMS concentration. The concentration of PVMDMS was varied between 10 to 50 wt.%. The amount of PVP was varied between 0.2 to 5 wt.%. Figure 26 shows the electrospinning results of KSH1-48 and KSH30-18 at 10 and 50 wt.% concentration of these polymers in the PVP mixture where the concentration of PVP varied between 0.2, 2 and 5 wt.%. Both tested PVMDMS samples showed fiber formation for a concentration of 10 wt.%. However, the important role of PVP as carrier polymer becomes also immediately clear.

The preparation of fibers was successful for both PVMDMS samples at 10 wt.% and a share of 5 wt.% PVP. Interestingly, the fiber diameter of KSH30-18 (10 wt.%) with 5 wt.% PVP almost doubled compared to the sample KSH10-48 processed in the same proportions and the same electrospinning spinning parameters. Both PVMDMS samples exhibited fiber fragment formation when 2 wt.% PVP was employed. Interestingly, 50 wt.% KSH1-48 and KSH30-18 did not result in fiber formation compared to 10 wt.% PVMDMS in the mixture. Droplet formation was seen with 50 wt.% KSH1-48 and all the PVP concentrations employed. However, the mixture of 50 wt.% KSH1-48 and 2 wt.% PVP gave some jet-like structures but also fiber fragments. Similar results were achieved with 50 wt.% KSH30-18 at 2 wt.% PVP as well as 5 wt.% PVP. Initially, a higher probability for successful fiber formation was assumed for solutions containing 50 wt.% KSH30-18 because of the possible polymer chain entanglements with increased concentration of the polymer in the solution. However, the electrospinning gave only few fiber fragments. To conclude in this particular case, the polymer-polymer interactions have to be taken into account. E.g. hydrogen-bonding between polyamide chains is an example of polymer-polymer interaction influencing viscosity and thus electrospinning as was reported in the literature. [39]

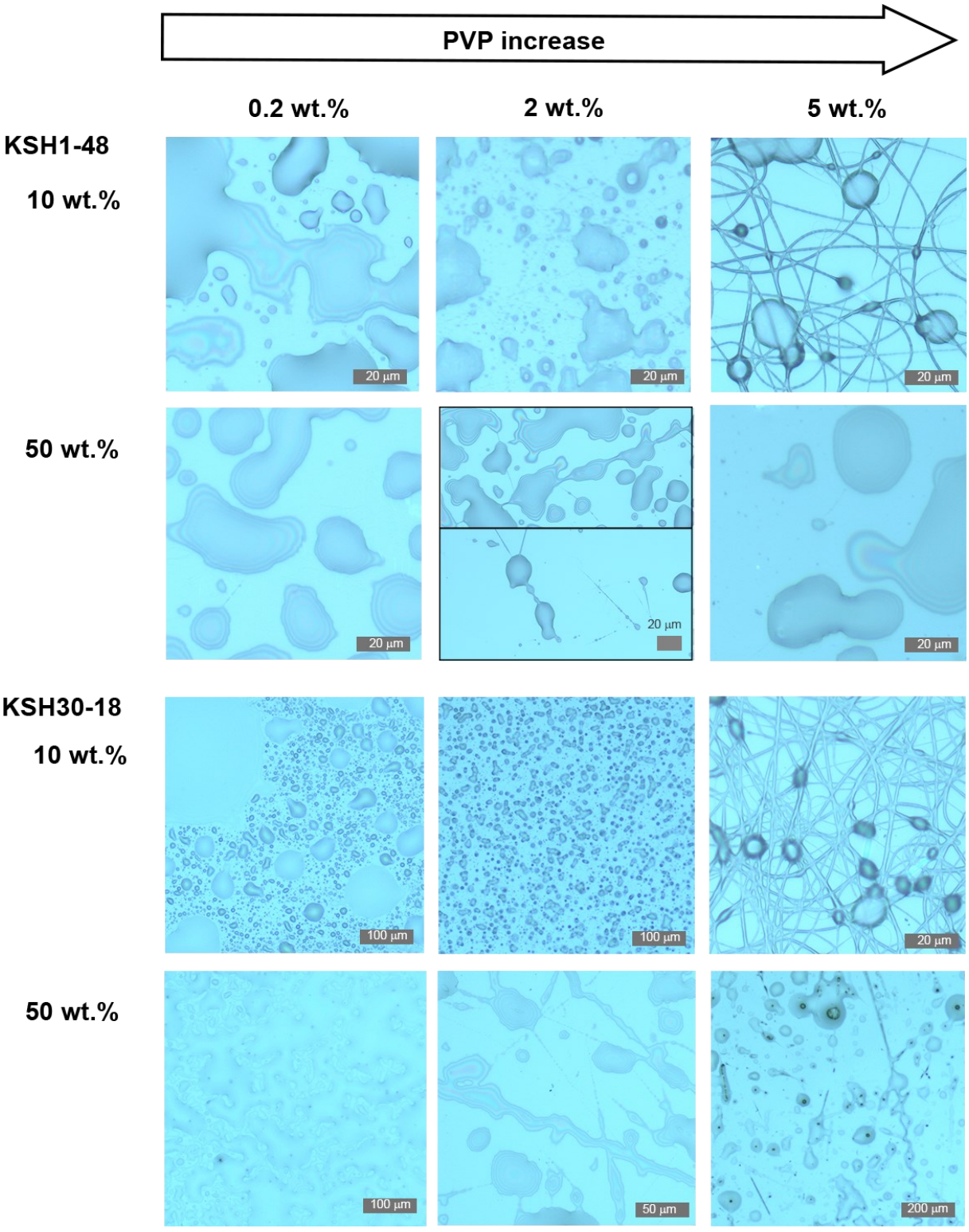

Figure 26: Microscopy images of electrospinning results of PVMDPS and PVP mixtures.

5.4 Stabilization of fibers via sol-gel processing

So far all concepts were based on 2D silicone-type crosslinking and fiber formation had to rely on entanglements. A more suitable approach towards stable fibers is generation of 3D connectivity, by e.g. chemical reaction of alkoxysilyl groups via sol-gel processes. The major questions to be answered are whether the alkoxygroups are in principle available for sol-gel processing, the best timing for the hydrolysis and condensation reactions, the degree of 3D connectivity that is needed. With that the question comes up, how sol-gel processing is induced: acid or base catalyzed, composition of mixture in regard to concentration of precursor and water.

Processing of pure PVMDMS / MeOH solutions via electrospinning, as described in Chapter 5.2, did show the challenges in fiber formation. It was assumed that pure PVMDMS – as a silicone type polymer – has not reached an optimum entanglement maybe due to the low molecular weight of the synthetized PVMDMS or to the fact that there are only very weak interactions between the polymer chains (as expected for silicones). [59] The idea now was to use sol-gel processing to hydrolyse and condense the pendant methoxy groups of PVMDMS to form siloxane connections between the chains. Therefore, the number of entanglements in the system could be increased, and with that a better spinnability is expected.

Sol-gel processing can lead to 3D structures as represented by a gel, however that depends on the applied processing parameters. For the electrospinning process only only liquids (in this case the sol) can be utilized. The 3D network slowly grows over the time as the hydrolysis and condensation reaction proceeds. Therefore the gelation time of a sol is a good phenomenological indicator of the rates of the underlying condensation reactions. For that reason, a detailed investigation of the gelation time in dependence of the pH value was performed. It is expected – as explained in Chapter 1.3 – that acidic conditions will give linear structures. Therefore, the range of pH values was varied from 0 to 6 (see Section 5.4.1). Another important parameter is the aging time. Hydrolysis and condensation reactions will proceed until all alkoxy groups are consumed. Thus, the timing for further processing has to be investigated (see Section 5.4.2).

5.4.1 Gelation time dependence

The studied polymers were KSH1-48, KSH3-48, KSH5-18, KSH10-48, KSH30-18. The dependencies of the gelation time on the pH value for different R values (water/silane ratio) 1, 3 and 6 ratio are depicted in Figure 27, Figure 28 and Figure 29, respectively. More detailed information can be found in the Appendix. Figure 30 shows the combined dependence of the three studied parameters, namely gelation time, pH and H_2O/Si ratio and KSH1-48, KSH10-48 and KSH30-18 are displayed by colored planes. Interestingly, the trend of gelation for each polymer did not change with the variation in H_2O/Si ratio. All samples gelled within three weeks; polymer KSH1-48 has always the highest gelation times regardless of the R value.

KSH30-18 exhibited the second highest gelation times. Polymers KSH3-48, KSH5-48 and KSH10-48 showed very similar gelation times regardless on R and therefore curves in the Figure 27, Figure 28 and Figure 29 are overlapped. Figure 31 gives the dependence of the gelation time on the pH value for KSH30-18 (20 wt.%) and the data were fitted with an exponential curve. The exponential fitting was assessed as a very good correlation to the experimental data represented by a correlation coefficient R = 1. Based on the hydrolysis and condensation reactions in the acidic environment, reaction rates correspond to the kinetics of the sol-gel processing in the acidic environment. An increase in pH leads to rapid rise in the gelation time which was experimentally confirmed on the PVMDMS system in this case. [17]

Polymers KSH1-48 and KSH30-18 were studied in detail and the gelation time dependence on pH for R = 1, 3, 6 is depicted in Figure 32. Figure 32 shows distinct differences between the dependence of the gelation time on R and the correlation between two polymers. The data show that the polymers KSH1-48 and KSH30-18 give the same trend in regard to R. The higher R is, the higher the gelation time becomes. An increase in R always revealed an extension of gelation time for all studied polymers. Faster gelation appeared in KSH30-18 compared to KSH1-48. According to the M_n as evaluated by NMR, KSH30-18 roughly consists of the same number of repeating units as KSH1-48. However, KSH30-18 might have a higher PDI due to the FRP chain transfers and hence consists of shorter and longer chains which can significantly alter the sol-gel transition. The difference in PDI can play a critical role during the sol-gel processing due to the presence of shorter and longer chains next to each other as Macon et al. reported for the gelation time of polyalkoxymethacrylate. Macon et al. investigated the chances in gelation time with regard to the molecular weight of the polymer as well as the PDI, which was found to be a significant factor rapidly decreasing the gelation time as the PDI increased. As molecular weight increased, gelation time decreased linearly in the system of polyalkoxymethacrylate. To conclude, the higher molecular weight leads to cross-linking within the network and therefore has an impact in the increase of gelation time. A correlation between gelation time and molecular weight was made and it was suggested that the gelation of such hybrids follows the bond percolation theory. Polymeric chains are crosslinked randomly in the system and form bigger lattices during the transition from sol to gel. The gel is observed as macroscopic gelation where a certain critical value for the lattice is reached. In a polydisperse system with shorter and longer chains, the longer chains form bigger lattices from the beginning of the sol-gel transition and contribute to the decrease in the gelation time. [8]

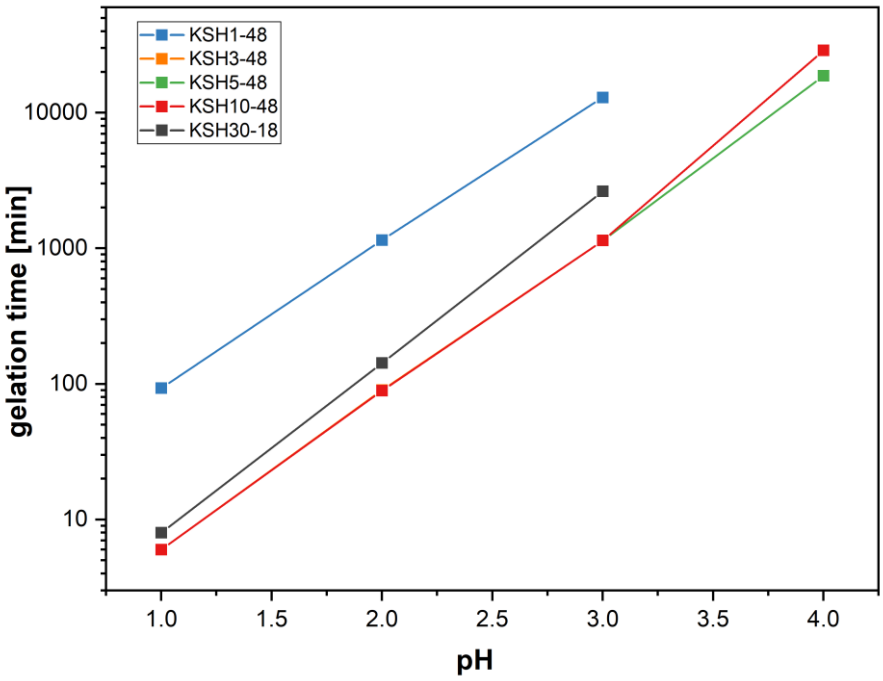

Figure 27: Gelation time versus pH value; comparison of all investigated polymers, R = 1.

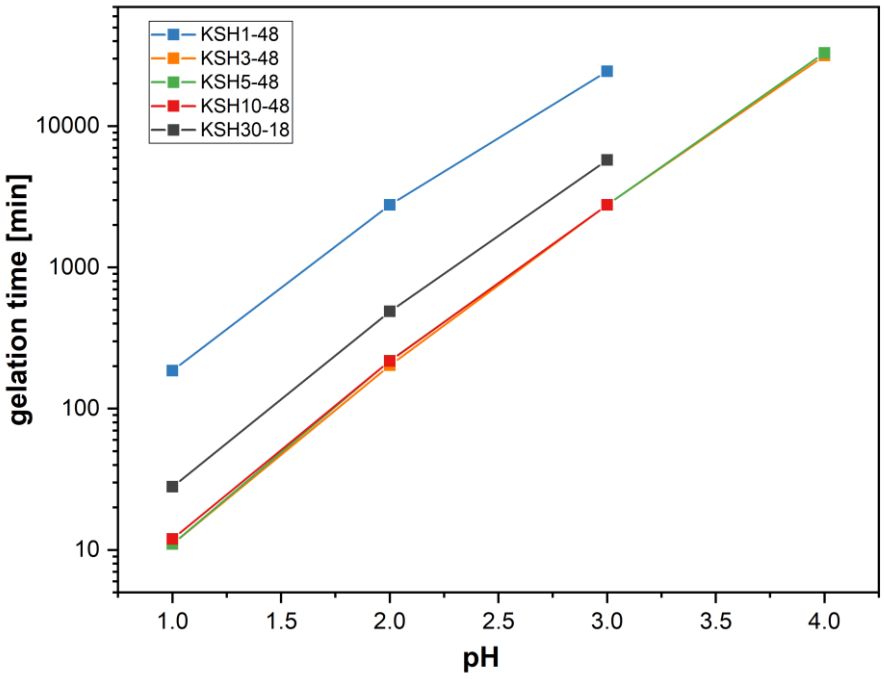

Figure 28: Gelation time versus pH value; comparison of all investigated polymers, R = 3.

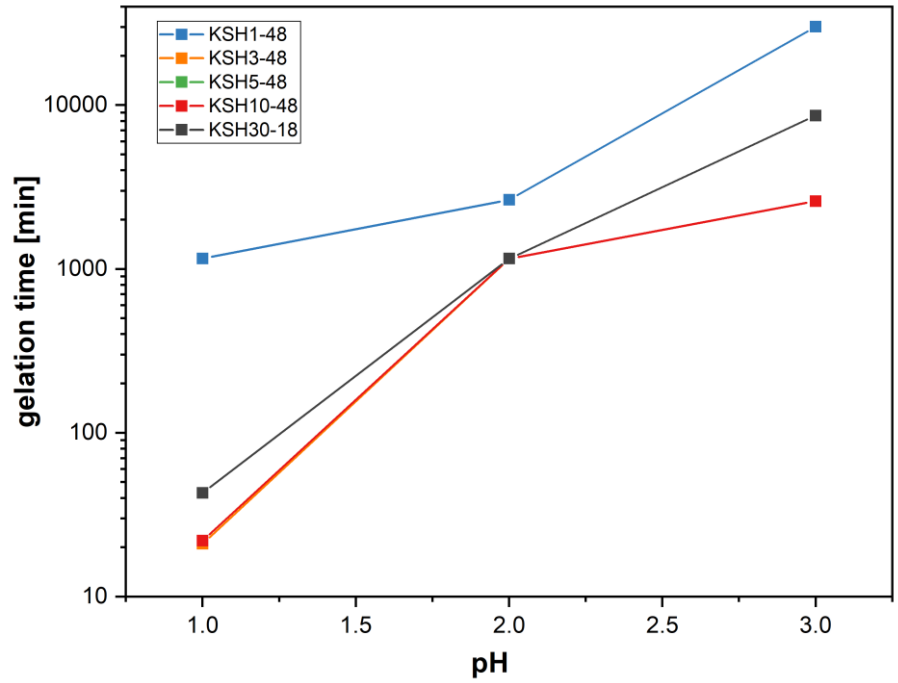

Figure 29: Gelation time versus pH value; comparison of all investigated polymers, R = 6.

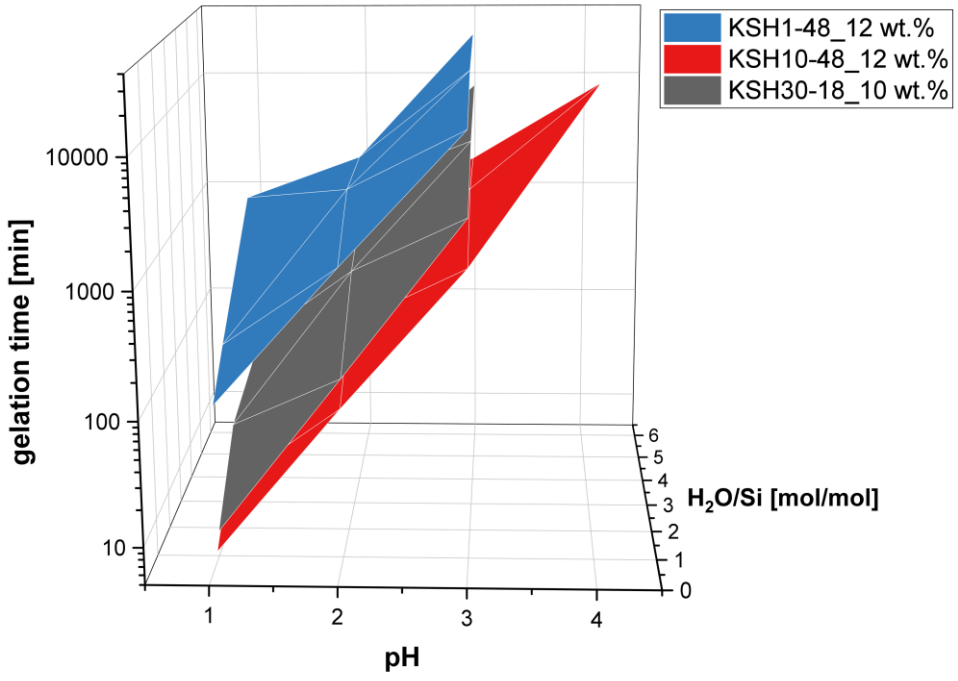

Figure 30: Combined dependence of the three studied parameters, namely gelation time, pH and H_2O/Si ratio for polymers KSH1-48, KSH10-48 and KSH30-18.

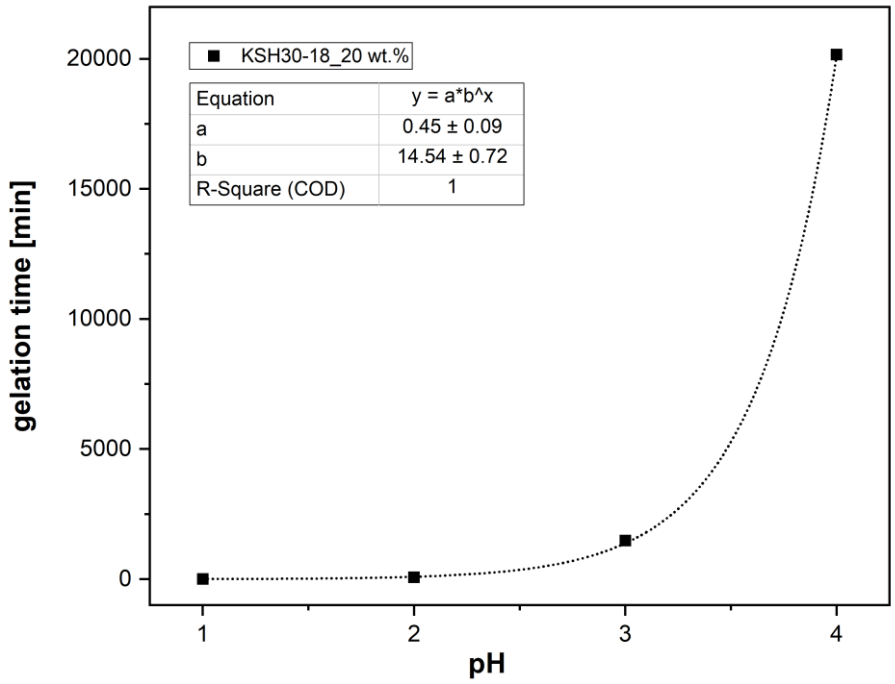

Figure 31: Gelation dependence on pH for 20wt.% KSH30-18 in various pH solutions fitted with an exponential curve.

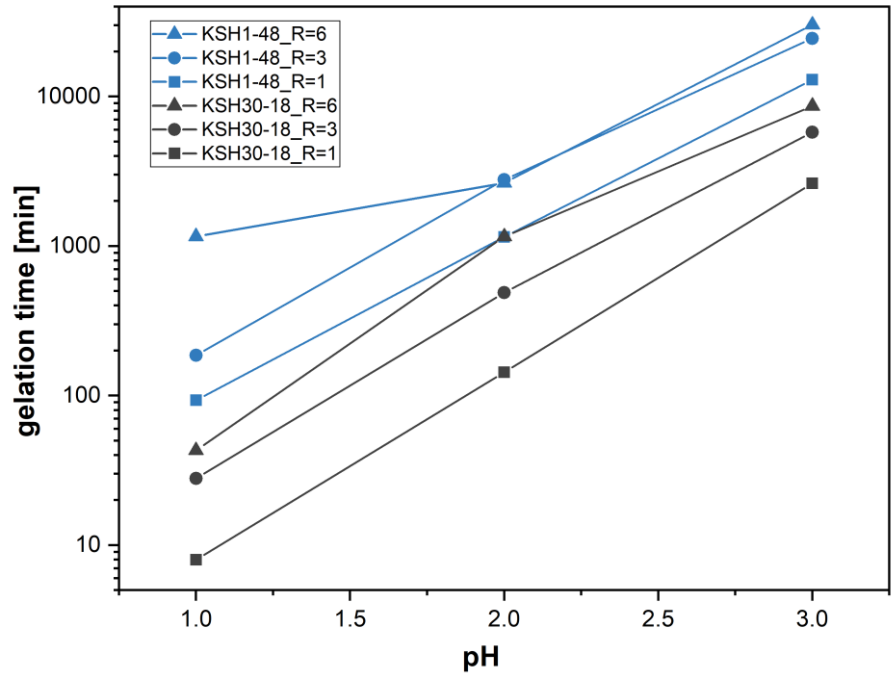

Figure 32: Gelation time versus pH value; comparison of KSH1-48 and KSH30-18, R = 1, 3, 6 for polymer.

5.4.2 Electrospinning dependence on the aging stage

With respect to the data achieved from the gelation time experiments reported in the Chapter 5.4.1, an appropriate composition of the PVMDMS solution was chosen, specifically KSH1-48 (12 wt.%) at pH = 1, R = 3; KSH1-48 (36 wt.%) at pH = 3, R = 3; KSH30-18 (30 wt.%) at pH = 3, R = 3. These solutions were subjected to the electrospinning process. The time after addition of the catalyst to the sol, has a very strong influence on the degree of condensation. Condensation reactions are continuously progressing and with that particles and network formation proceeds simultaneously. Organoalkoxysilanes, such as PVMDMS, behave differently than TEOS during sol-gel reactions upon pH, as was described in Chapter 1.3, due to the electronic effects of the side groups. Holubová et al. reported that a solution is spinnable if hydrolysis is suppressed against condensation reaction, specifically for the organosilane system. As a result, the 3D structure is forming slowly due to a lack of hydrolyzed groups capable of condensation reaction. As the sol-gel reactions proceed, the viscosity of the sol increases. The suppression of the hydrolysis prevents premature gelation of the electrospinning solution which can emerge and result in gel formation as an unsuitable working conditions for electrospinning. [5]

The overall results of the electrospinning for various aging times are depicted in Figure 33. KSH1-48 and KSH30-18 were chosen for a more detailed study. The aging time was varied from 15 min to 4.5 hr. Based on the obtained data, further condensation reactions with time contributed to the 3D structure and the formation of fiber-like structures was achieved. Early stages of aging resulted in particle formation in all of the studied samples as it is depicted in Figure 33.

KSH1-48 (12 wt.%) at pH = 1, R = 3 was subjected to electrospinning. The amount of material – as already represented by the low concentration of PVMDMS – was probably too low for fiber formation. Aligned structures of separated particles resulted from the electrospinning process. Higher concentrations of PVMDMS were chosen in order to investigate influence of the polymer concentration on the electrospinning product. Therefore, KSH1-48 (36 wt.%) at pH = 3, R = 3 was subjected to electrospinning and as a result, fiber fragments with a diameter of roughly 2 μm were obtained.

A higher concentration was chosen with KSH30-18 (30 wt.%) at pH = 3, R = 3. In addition, this precursor shows a higher molecular weight leading to better entanglements in the electrospinning solution. Fiber fragments were obtained in a late stage of aging and these fiber fragments have diameter of approximately 5 μm.

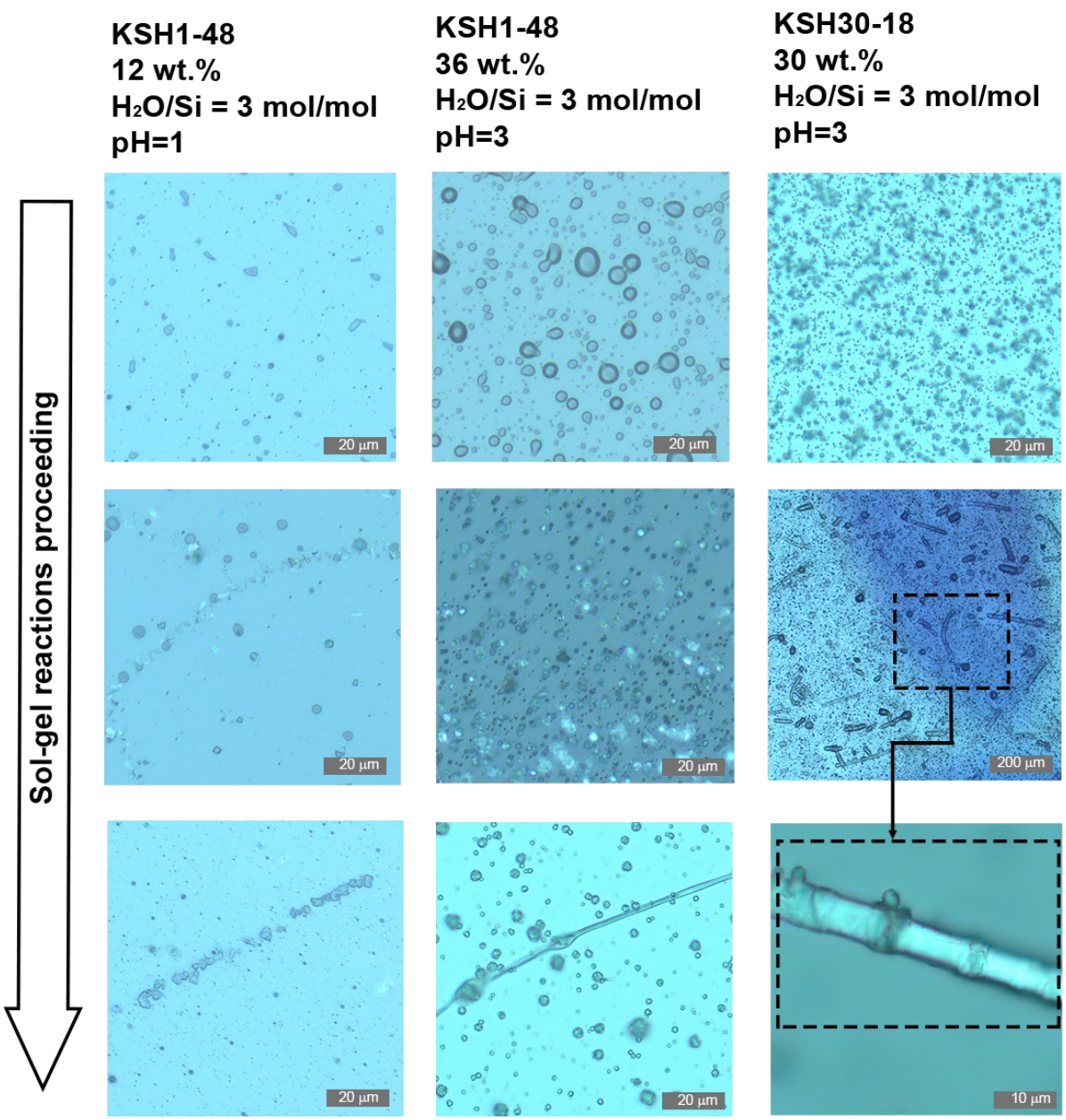

Figure 33: Microscopy images of fibers spun from acidic PVMDMS solutions in MeOH ; the aging time was varied from 15 min to 4.5 hr.

6 CONCLUSION

Polyorganosilanes seem to be promising novel precursor materials for the production of fibers using the electrospinning technique. Because of the versatile chemistry offered by these precursors, polyorganosilane-derived fibers might reveal new sets of properties and thereby enable innovations for nowadays life. Polyorganosilanes have been investigated for various different purposes and applications by other groups but there are no publications available demonstrating electrospinning of these precursors. [4]

The overall aim of the present work was the preparation of fibers via electrospinning applying poly(vinylmethyldimethoxysilane) as a precursor molecule. Since this has not been demonstrated before, the initial experiments were focused on the nature of this precursor polymer. Criticial parameters potentially affecting the final fiber formation capabilities, such as molecular weight or degree of polymerization as well as solubility had to be elucidated prior to the electrospinning itself. A free-radical polymerization technique was utilized for the purpose of PVMDMS preparation. Different rates of the propagation reaction during FRP with the aim to synthesize polymers of various molecular weights were investigated by variation of the radical starter concentration. Successful polymerization was confirmed by detailed FT-IR spectroscopic assessment. NMR spectroscopic analysis was performed to determine the molecular weight of the polymer, specifically the number-average molecular weight via quantification of the chain end-groups. It was expected due to the nature of the FRP that different end groups will be present in the polymer. However, the NMR analysis was not sufficiently sensitive to detect all end-groups. Thus, it was only possible to estimate a trend of increasing M_w with increasing concentration of initiator. However, a quantitative statement about the number average degree of polymerization would be possible once the terminal methyl group can be unambiguously assigned to a specific chemical shift in the 2D-NMR data.

First electrospinning experiments were performed with solutions of pure PVMDMS in a solvent, specifically in methanol. All parameters for the electrospinning process had to be identified for the first time. Only few fiber fragments at very high concentration of PVMDMS could be obtained. The system tended to form droplets and coatings on the collector most likely due to insufficient number of chain entanglements in the electrospinning solution. An indication which supports this assumption is that the polymer with the putatively highest PDI was the most successful in fiber formation.

It was also anticipated that the degree of entanglement as well as the strength of mutual interaction between interlocking chains would not provide the necessary conditions allowing stable fiber formation. Therefore, two different additional strategies aiming to enhance fiber formation were pursued. On the one hand, a carrier polymer can be used to aid the formation of poly(vinylmethyldimethoxysilane) based fibers. On the other hand, residual alkoxy moieties can be condensed to increase the degree of crosslinking in the prepolymer via the formation of siloxane bonds.

Polyvinylpyrrolidone, as a well established polymer in electrospinning processes, was used for the purpose of facilitating fiber formation with a carrier polymer. It can be stated that the addition of PVP enhances the spinnability of PVMDMS as a very general conclusion. Fibers were successfully prepared from blends of PVMDMS and PVP where fiber diameters varied from 100 nm to 1 µm strongly depending on the molecular weight of PVMDMS.

As another way to improve fiber formation, sol-gel processing was applied with the aim to induce crosslinking of the macromolecules and therefore increase the number of entanglements per molecule. PVMDMS consists of repeating vinylmethyldimethoxysilane units, a molecule bearing two methoxygroups capable of hydrolysis and condensation. These reactions will give siloxane bonds within the material, specifically between the chains of PVMDMS gradually increasing the molecular weight which is characteristic for sol-gel processes. The process was carefully investigated with respect to identification of the optimal pH value and aging time. Both parameters are of crucial importance because they influence the degree of condensation of the sol, which again is responsible for the viscosity and crosslinking of the polymer network (solution). Electrospinning of prepolymerized and precondensed PVMDMS showed the formation of small fiber fragments. The macromolecular structure of the polymeric precursor as well as the precursor concentration seem to be the most important parameters with respect to the product quality. While an insufficient amount of material resulted in formation of particle-like structures in the aligned shape from the jet, an increase of the PVMDMS content enhanced fiber formation and consequently fragments of fibers were achieved. In addition, longer ageing seems to be beneficial for fiber formation.

In summary, successful fiber formation with PVMDMS was shown for the first time. It was found that stable fiber formation with the obtained polymers is not achievable, presumably due to the low molecular weight and the associated low entanglement number per macromolecule. However, fibers could successfully be prepared by the addition of a carrier polymer such as polyvinylpyrrolidone to the spinning solution. In addition, further polymerization of PVMDMS to yield siloxane crosslinks by hydrolysis and condensation, in a sol-gel type fashion, seems to be a very promising approach for electrospinning. In the latter case, further investigations are necessary to investigate the plethora of different processing parameters.

7 LITERATURE

[1] XUE, Jiajia, WU, Tong, DAI, Yunqian and XIA, Younan. *Electrospinning and Electrospun Nanofibers: Methods, Materials, and Applications*. *Chemical Reviews* [online]. 24 April 2019. Vol. 119, no. 8, p. 5298–5415. DOI 10.1021/acs.chemrev.8b00593. Available from: https://pubs.acs.org/doi/10.1021/acs.chemrev.8b00593

[2] TUCKER, Nick, STANGER, Jonathan J, STAIGER, Mark P, RAZZAQ, Hussam and HOFMAN, Kathleen. *The history of the science and technology of electrospinning from 1600 to 1995*. *Journal of Engineered Fibers and Fabrics* [online]. 15 June 2012. Vol. 7, no. 3, p. 63–73. DOI 10.1177/155892501200702s10. Available from: http://www.jeffjournal.org

[3] ZU, Guoqing, KANAMORI, Kazuyoshi, SHIMIZU, Taiyo, ZHU, Yang, MAENO, Ayaka, KAJI, Hironori, NAKANISHI, Kazuki and SHEN, Jun. *Versatile Double-Cross-Linking Approach to Transparent, Machinable, Supercompressible, Highly Bendable Aerogel Thermal Superinsulators*. *Chemistry of Materials*. 2018. Vol. 30, no. 8, p. 2759–2770. DOI 10.1021/acs.chemmater.8b00563.

[4] XU, Yunxia, WEN, Yuquan, WU, Yi Nan, LIN, Changxu and LI, Guangtao. *Hybrid nanofibrous mats with remarkable solvent and temperature resistance produced by electrospinning technique*. *Materials Letters* [online]. 2012. Vol. 78, p. 139–142. DOI 10.1016/j.matlet.2012.03.016. Available from: http://dx.doi.org/10.1016/j.matlet.2012.03.016

[5] HOLUBOVÁ, Barbora, MÁKOVÁ, Veronika, MÜLLEROVÁ, Jana, BRUS, Jiří, HAVLÍČKOVÁ, Kristýna, JENČOVÁ, Věra, MICHALCOVÁ, Alena, KULHÁNKOVÁ, Johana and ŘEZANKA, Michal. *Novel chapter in hybrid materials: One-pot synthesis of purely organosilane fibers*. *Polymer*. 2 March 2020. Vol. 190. DOI 10.1016/j.polymer.2020.122234.

[6] NOVAK, Bruce M. *Hybrid Nanocomposite Materials?between inorganic glasses and organic polymers*. *Advanced Materials* [online]. June 1993. Vol. 5, no. 6, p. 422–433. DOI 10.1002/adma.19930050603. Available from: http://doi.wiley.com/10.1002/adma.19930050603

[7] MALUCELLI, Giulio. *Hybrid Organic/Inorganic Coatings Through Dual-Cure Processes: State of the Art and Perspectives*. *Coatings* [online]. 2 March 2016. Vol. 6, no. 1, p. 10. DOI 10.3390/coatings6010010. Available from: http://www.mdpi.com/2079-6412/6/1/10

[8] MAÇON, Anthony L.B., KASUGA, Toshihiro, REMZI BECER, C. and JONES, Julian R. *Silica/methacrylate class II hybrid: Telomerisation: vs. RAFT polymerisation*. *Polymer Chemistry*. 2017. Vol. 8, no. 23, p. 3603–3611. DOI 10.1039/c7py00516d.

[9] TOSKAS, Georgios, CHERIF, Chokri, HUND, Rolf Dieter, LAOURINE, Ezzedine, FAHMI, Amir and MAHLTIG, Boris. *Inorganic/organic (SiO2)/PEO hybrid electrospun nanofibers produced from a modified sol and their surface modification*

possibilities. *ACS Applied Materials and Interfaces*. 2011. Vol. 3, no. 9, p. 3673–3681. DOI 10.1021/am200858s.

[10] GELTMEYER, Jozefien, DE ROO, Jonathan, VAN DEN BROECK, Freya, MARTINS, José C., DE BUYSSER, Klaartje and DE CLERCK, Karen. *The influence of tetraethoxysilane sol preparation on the electrospinning of silica nanofibers*. *Journal of Sol-Gel Science and Technology*. 1 February 2016. Vol. 77, no. 2, p. 453–462. DOI 10.1007/s10971-015-3875-1.

[11] HÜSING, Nicola and SCHUBERT, Ulrich. *Aerogels—Airy Materials: Chemistry, Structure, and Properties*. *Angewandte Chemie International Edition*. 2 February 1998. Vol. 37, no. 1/2, p. 22–45. DOI 10.1002/1521-3773(19980202)37:1/2<22::aid-anie22>3.3.co;2-9.

[12] INNOCENZI, P., BRUSATIN, G. and BABONNEAU, F. *Competitive polymerization between organic and inorganic networks in hybrid materials*. *Chemistry of Materials*. 2000. Vol. 12, no. 12, p. 3726–3732. DOI 10.1021/cm001139b.

[13] INTERNATIONAL UNION OF PURE AND APPLIED CHEMISTRY. SUBCOMMITTEE ON POLYMER TERMINOLOGY., JONES, Richard G. and INTERNATIONAL UNION OF PURE AND APPLIED CHEMISTRY. COMMISSION ON MACROMOLECULAR NOMENCLATURE. *Compendium of polymer terminology and nomenclature : IUPAC recommendations, 2008*. Royal Society of Chemistry, 2009. ISBN 9780854044917.

[14] SU, Wei-Fang. *Radical Chain Polymerization*. In : *Radical Chain Polymerization.* 2013. p. 137–183. ISBN 978-3-642-38730-2.

[15] RAMAKRISHNAN, S. *Condensation Polymerization*. *Resonance* [online]. 2017. Vol. 22, no. 4, p. 355–368. DOI 10.1007/s12045-017-0475-0. Available from: https://doi.org/10.1007/s12045-017-0475-0

[16] SIVERGIN, Yu. M., KIREEVA, S. M. and GRISHINA, I. N. *Peroxides and Hydroperoxides as Polymerisation Initiators*. *International Polymer Science and Technology* [online]. 7 March 2003. Vol. 30, no. 3, p. 64–74. DOI 10.1177/0307174X0303000316. Available from: http://journals.sagepub.com/doi/10.1177/0307174X0303000316

[17] SCHUBERT, Ulrich and HÜSING, Nicola. *Synthesis of Inorganic Materials*. 4th editio. Weinheim : Wiley-VCH Verlag, 2019. ISBN 978-3-527-34457-4.

[18] ESPOSITO, Serena. *"Traditional" Sol-Gel Chemistry as a Powerful Tool for the Preparation of Supported Metal and Metal Oxide Catalysts*. *Materials* [online]. 23 February 2019. Vol. 12, no. 4, p. 668. DOI 10.3390/ma12040668. Available from: http://www.mdpi.com/1996-1944/12/4/668

[19] ISSA, Ahmed and LUYT, Adriaan. *Kinetics of Alkoxysilanes and Organoalkoxysilanes Polymerization: A Review*. *Polymers* [online]. 21 March 2019. Vol. 11, no. 3, p. 537. DOI 10.3390/polym11030537. Available from: https://www.mdpi.com/2073-4360/11/3/537

[20] DOSHI, Jayesh and RENEKER, Darrell H. *Electrospinning process and applications*

of electrospun fibers. *Journal of Electrostatics* [online]. August 1995. Vol. 35, no. 2–3, p. 151–160. DOI 10.1016/0304-3886(95)00041-8. Available from: https://linkinghub.elsevier.com/retrieve/pii/0304388695000418

[21] WU, Jing, WANG, Nü, ZHAO, Yong and JIANG, Lei. *Electrospinning of multilevel structured functional micro-/nanofibers and their applications*. *Journal of Materials Chemistry A*. 7 July 2013. Vol. 1, no. 25, p. 7290–7305. DOI 10.1039/c3ta10451f.

[22] GHORANI, Behrouz and TUCKER, Nick. *Fundamentals of electrospinning as a novel delivery vehicle for bioactive compounds in food nanotechnology*. *Food Hydrocolloids* [online]. 1 October 2015. Vol. 51, p. 227–240. DOI 10.1016/j.foodhyd.2015.05.024. Available from: https://linkinghub.elsevier.com/retrieve/pii/S0268005X15002258

[23] RENEKER, Darrell H. and YARIN, Alexander L. *Electrospinning jets and polymer nanofibers*. *Polymer* [online]. 13 May 2008. Vol. 49, no. 10, p. 2387–2425. DOI 10.1016/j.polymer.2008.02.002. Available from: https://linkinghub.elsevier.com/retrieve/pii/S0032386108001407

[24] FRENOT, Audrey and CHRONAKIS, Ioannis S. *Polymer nanofibers assembled by electrospinning*. *Current Opinion in Colloid & Interface Science* [online]. March 2003. Vol. 8, no. 1, p. 64–75. DOI 10.1016/S1359-0294(03)00004-9. Available from: https://linkinghub.elsevier.com/retrieve/pii/S1359029403000049

[25] IBRAHIM, Hassan M. and KLINGNER, Anke. *A review on electrospun polymeric nanofibers: Production parameters and potential applications*. *Polymer Testing* [online]. 1 October 2020. Vol. 90, p. 106647. DOI 10.1016/j.polymertesting.2020.106647. Available from: https://linkinghub.elsevier.com/retrieve/pii/S0142941820305298

[26] LOFGREEN, Jennifer E. and OZIN, Geoffrey A. *Controlling morphology and porosity to improve performance of molecularly imprinted sol–gel silica*. *Chem. Soc. Rev.* [online]. 7 February 2014. Vol. 43, no. 3, p. 911–933. DOI 10.1039/C3CS60276A. Available from: http://xlink.rsc.org/?DOI=C3CS60276A

[27] ZU, Guoqing, KANAMORI, Kazuyoshi, SHIMIZU, Taiyo, ZHU, Yang, MAENO, Ayaka, KAJI, Hironori, NAKANISHI, Kazuki and SHEN, Jun. *Versatile Double-Cross-Linking Approach to Transparent, Machinable, Supercompressible, Highly Bendable Aerogel Thermal Superinsulators*. *Chemistry of Materials*. 24 April 2018. Vol. 30, no. 8, p. 2759–2770. DOI 10.1021/acs.chemmater.8b00563.

[28] ZU, Guoqing, KANAMORI, Kazuyoshi, MAENO, Ayaka, KAJI, Hironori and NAKANISHI, Kazuki. *Superflexible Multifunctional Polyvinylpolydimethylsiloxane-Based Aerogels as Efficient Absorbents, Thermal Superinsulators, and Strain Sensors*. *Angewandte Chemie - International Edition*. 2018. Vol. 57, no. 31, p. 9722–9727. DOI 10.1002/anie.201804559.

[29] ZU, Guoqing, SHIMIZU, Taiyo, KANAMORI, Kazuyoshi, ZHU, Yang, MAENO, Ayaka, KAJI, Hironori, SHEN, Jun and NAKANISHI, Kazuki. *Ultralow-Cost , Highly Scalable , Transparent , Superflexible Doubly Crosslinked Polyvinylpolymethylsiloxane Aerogel Superinsulators*. . 2018.

[30] MIXER, R. Y. and BAILEY, D L. *The mode of peroxide-catalyzed polymerization of vinyltriethoxysilane*. *Journal of Polymer Science* [online]. December 1955. Vol. 18, no. 90, p. 573–582. DOI 10.1002/pol.1955.120189013. Available from: http://doi.wiley.com/10.1002/pol.1955.120189013

[31] SUN, Haixiang, XU, Yanyan, ZHOU, Yingying, GAO, Wen, ZHAO, Haoru and WANG, Wenguang. *Preparation of superhydrophobic nanocomposite fiber membranes by electrospinning poly(vinylidene fluoride)/silane coupling agent modified SiO2 nanoparticles*. *Journal of Applied Polymer Science*. 2017. Vol. 134, no. 13, p. 1–8. DOI 10.1002/app.44501.

[32] LI, Lichun, YALCIN, Baris, NGUYEN, Baochau N., MEADOR, Mary Ann B. and CAKMAK, Miko. *Flexible nanofiber-reinforced aerogel (Xerogel) synthesis, manufacture, and characterization*. *ACS Applied Materials and Interfaces*. 2009. Vol. 1, no. 11, p. 2491–2501. DOI 10.1021/am900451x.

[33] MOBIN, Rizwana, RANGREEZ, Tauseef Ahmad, CHISTI, Hamida Tun Nisa, INAMUDDIN and REZAKAZEMI, Mashallah. *Organic-Inorganic Hybrid Materials and Their Applications*. . 2019. P. 1135–1156. DOI 10.1007/978-3-319-95987-0_33.

[34] CHRISTIANSEN, Lasse and FOJAN, Peter. *Solution electrospinning of particle-polymer composite fibres*. *Manufacturing Review*. 2016. Vol. 3. DOI 10.1051/mfreview/2016013.

[35] ZU, Guoqing, SHIMIZU, Taiyo, KANAMORI, Kazuyoshi, ZHU, Yang, MAENO, Ayaka, KAJI, Hironori, SHEN, Jun and NAKANISHI, Kazuki. *Transparent, Superflexible Doubly Cross-Linked Polyvinylpolymethylsiloxane Aerogel Superinsulators via Ambient Pressure Drying*. *ACS Nano*. 2018. Vol. 12, no. 1, p. 521–532. DOI 10.1021/acsnano.7b07117.

[36] REZAEI, Sasan, JALALI, Amirjalal, ZOLALI, Ali M., ALSHRAH, Mohammed, KARAMIKAMKAR, Solmaz and PARK, Chul B. *Robust, ultra-insulative and transparent polyethylene-based hybrid silica aerogel with a novel non-particulate structure*. *Journal of Colloid and Interface Science*. 15 July 2019. Vol. 548, p. 206–216. DOI 10.1016/j.jcis.2019.04.028.

[37] ABUTALEB, Ahmed, LOLLA, Dinesh, ALJUHANI, Abdulwahab, SHIN, Hyeon U., RAJALA, Jonathan W. and CHASE, George G. *Effects of surfactants on the morphology and properties of electrospun polyetherimide fibers*. *Fibers*. 1 September 2017. Vol. 5, no. 3. DOI 10.3390/fib5030033.

[38] HUANG, Chao and THOMAS, Noreen L. *Fabrication of porous fibers via electrospinning: strategies and applications*. *Polymer Reviews* [online]. 15 November 2019. P. 1–53. DOI 10.1080/15583724.2019.1688830. Available from: https://www.tandfonline.com/doi/full/10.1080/15583724.2019.1688830

[39] SHENOY, Suresh L., BATES, W. Douglas, FRISCH, Harry L. and WNEK, Gary E. *Role of chain entanglements on fiber formation during electrospinning of polymer solutions: Good solvent, non-specific polymer-polymer interaction limit*. *Polymer*. 25 April 2005. Vol. 46, no. 10, p. 3372–3384. DOI 10.1016/j.polymer.2005.03.011.

[40] DE GENNES, P. G. *Reptation of a Polymer Chain in the Presence of Fixed Obstacles*. *The Journal of Chemical Physics* [online]. 15 July 1971. Vol. 55, no. 2, p. 572–579. DOI 10.1063/1.1675789. Available from: http://aip.scitation.org/doi/10.1063/1.1675789

[41] MAEDA, Tomohiro, KIM, Young Jin, AOYAGI, Takao and EBARA, Mitsuhiro. *The design of temperature-responsive nanofiber meshes for cell storage applications*. *Fibers*. 1 March 2017. Vol. 5, no. 1. DOI 10.3390/fib5010013.

[42] MUNIR, Muhammad Miftahul, SURYAMAS, Adi Bagus, ISKANDAR, Ferry and OKUYAMA, Kikuo. *Scaling law on particle-to-fiber formation during electrospinning*. *Polymer*. 23 September 2009. Vol. 50, no. 20, p. 4935–4943. DOI 10.1016/j.polymer.2009.08.011.

[43] LI, Lu, JIANG, Zhao, LI, Mengmeng, LI, Ruosong and FANG, Tao. *Hierarchically structured PMMA fibers fabricated by electrospinning*. *RSC Advances*. 2014. Vol. 4, no. 95, p. 52973–52985. DOI 10.1039/c4ra05385k.

[44] ZUO, Weiwei, ZHU, Meifang, YANG, Wen, YU, Hao, CHEN, Yanmo and ZHANG, Yu. *Experimental study on relationship between jet instability and formation of beaded fibers during electrospinning*. *Polymer Engineering and Science*. May 2005. Vol. 45, no. 5, p. 704–709. DOI 10.1002/pen.20304.

[45] WACKERLY, Jay Wm and DUNNE, James F. *Synthesis of Polystyrene and Molecular Weight Determination by 1H NMR End-Group Analysis*. *Journal of Chemical Education*. 14 November 2017. Vol. 94, no. 11, p. 1790–1793. DOI 10.1021/acs.jchemed.6b00814.

[46] ZU, Guoqing, SHIMIZU, Taiyo, KANAMORI, Kazuyoshi, ZHU, Yang, MAENO, Ayaka, KAJI, Hironori, SHEN, Jun and NAKANISHI, Kazuki. *Transparent, Superflexible Doubly Cross-Linked Polyvinylpolymethylsiloxane Aerogel Superinsulators via Ambient Pressure Drying*. *ACS Nano*. 23 January 2018. Vol. 12, no. 1, p. 521–532. DOI 10.1021/acsnano.7b07117.

[47] LI, Ying Sing, BA, Abdul and MAHMOOD, Maleeha S. *Infrared and Raman spectra of triacetoxyvinylsilane, aqueous sol-gel and xerogel*. *Spectrochimica Acta - Part A: Molecular and Biomolecular Spectroscopy*. April 2009. Vol. 72, no. 3, p. 605–609. DOI 10.1016/j.saa.2008.10.055.

[48] NGUYEN, Van, YOSHIDA, Wayne and COHEN, Yoram. *Graft polymerization of vinyl acetate onto silica*. *Journal of Applied Polymer Science* [online]. 10 January 2003. Vol. 87, no. 2, p. 300–310. DOI 10.1002/app.11376. Available from: http://doi.wiley.com/10.1002/app.11376

[49] LI, Ying Sing, WRIGHT, Paul B., PURITT, Rosalyn and TRAN, Tuan. *Vibrational spectroscopic studies of vinyltriethoxysilane sol-gel and its coating*. *Spectrochimica Acta - Part A: Molecular and Biomolecular Spectroscopy*. October 2004. Vol. 60, no. 12, p. 2759–2766. DOI 10.1016/j.saa.2003.12.047.

[50] HATADA, Koichi, KITAYAMA, Tatsuki, UTE, Koichi, TERAWAKI, Yoshio and YANAGIDA, Takatsune. *End-group analysis of poly(methyl methacrylate) prepared*

with benzoyl peroxide by 750 MHz high-resolution 1H NMR spectroscopy. *Macromolecules*. 1997. Vol. 30, no. 22, p. 6754–6759. DOI 10.1021/ma970672i.

[51] SPERLING, L.H. *Introduction to Physical Polymer Science* [online]. Wiley, 2005. ISBN 9780471706069. Available from: https://onlinelibrary.wiley.com/doi/book/10.1002/0471757128

[52] RUDIN, Alfred and CHOI, Phillip. *Free-Radical Polymerization*. In : *The Elements of Polymer Science & Engineering* [online]. Elsevier, 2013. p. 341–389. Available from: https://linkinghub.elsevier.com/retrieve/pii/B9780123821782000080

[53] BRAUN, Dietrich, CHERDRON, Harald and RITTER, Helmut. *Introduction*. In : *Polymer Synthesis: Theory and Practice* [online]. Berlin, Heidelberg : Springer Berlin Heidelberg, 2001. p. 1–33. ISBN 0471166286. Available from: http://link.springer.com/10.1007/978-3-662-04573-2_1

[54] JIANG, Qimin, LI, Jiating, HUANG, Wenyan, ZHANG, Dongliang, CHEN, Jianhai, YANG, Hongjun, XUE, Xiaoqiang and JIANG, Bibiao. *Radical polymerization in the presence of a peroxide monomer: An approach to branched vinyl polymers*. *Polymer Chemistry*. 14 August 2017. Vol. 8, no. 30, p. 4428–4439. DOI 10.1039/c7py00844a.

[55] SCORAH, Matthew J., COSENTINO, Renato, DHIB, Ramdhane and PENLIDIS, Alexander. *Experimental study of a tetrafunctional peroxide initiator: Bulk free radical polymerization of butyl acrylate and vinyl acetate*. *Polymer Bulletin*. 2006. Vol. 57, no. 2, p. 157–167. DOI 10.1007/s00289-006-0547-x.

[56] INTERNATIONAL ORGANIZATION FOR STANDARDIZATION. *Particle size analysis - Dynamic light scattering (DLS)*. 2nd. Geneva : ISO 22412:2017(E), 2017.

[57] NARTETAMRONGSUTT, Kitchaporn and CHASE, George G. *The influence of salt and solvent concentrations on electrospun polyvinylpyrrolidone fiber diameters and bead formation*. *Polymer*. 3 April 2013. Vol. 54, no. 8, p. 2166–2173. DOI 10.1016/j.polymer.2013.02.028.

[58] WANG, Shu Qiang, HE, Ji Huan and XU, Lan. *Non-ionic surfactants for enhancing electrospinability and for the preparation of electrospun nanofibers*. *Polymer International*. September 2008. Vol. 57, no. 9, p. 1079–1082. DOI 10.1002/pi.2447.

[59] ZHU, Ai-jun and STERNSTEIN, S S. *Nonlinear viscoelasticity of nanofilled polymers : interfaces , chain statistics and properties recovery kinetics*. . 2003. Vol. 63, p. 1113–1126. DOI 10.1016/S0266-3538(03)00032-0.

8 LIST OF ABBREVIATIONS AND SYMBOLS

2D	two-dimensional
3D	three-dimensional
AC	alternating current
Ar	argon gas
ATR	attenuated total reflectance
D4	deuterium
Da	unit Dalton
DC	direct current
DI	deionized water
DLS	dynamic light scattering
DP	degree of polymerization
FT-IR	Fourier transform infrared spectroscopy
G	gauge
hr	hours
l	liquid
MeOH	methanol
min	minutes
mL	milliliter
M_n	number-average molecular weight
mol.	molar concentration
M_w	weight-average molecular weight
PDI	polydispersity index
PMMA	poly(methylmethacrylate)
PVMDMS	poly(vinylmethyldimethoxysilane)
PVP	poly(vinylpyrrolidone)
R	molar ratio water to silane
rpm	revolutions per minute
s	solid
SEC	size-exclusion chromatography
SEM	scanning electron microscope
TEOS	tetraethylorthosilicate
TEOS	tetraethoxysilane
V	voltage
VMDMS	vinylmethyldimethoxysilane
wt.	weight concentration

9 APPENDIX

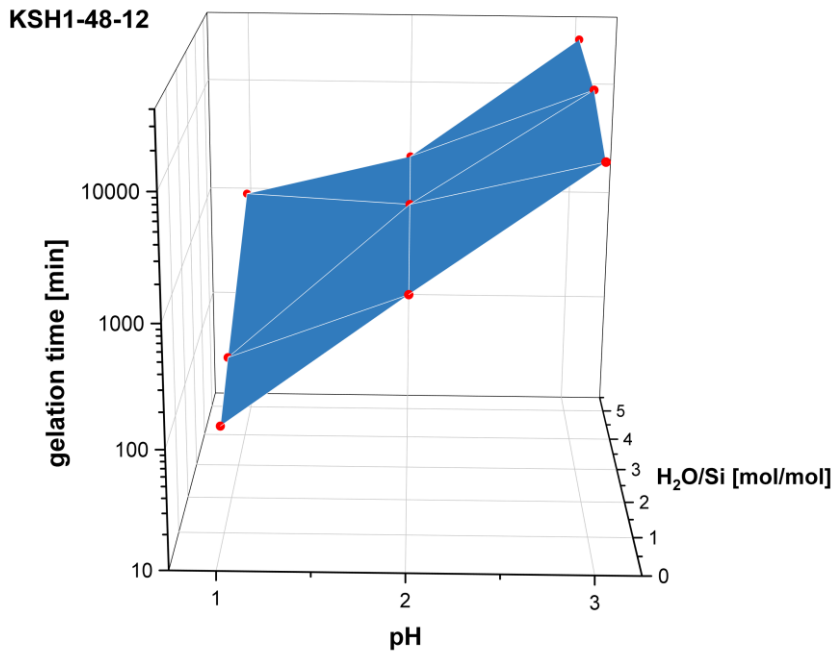

Figure 34: Combined dependence of the three studied parameters, namely gelation time, pH and H_2O/Si ratio for polymers KSH1-48 (12 wt.%).

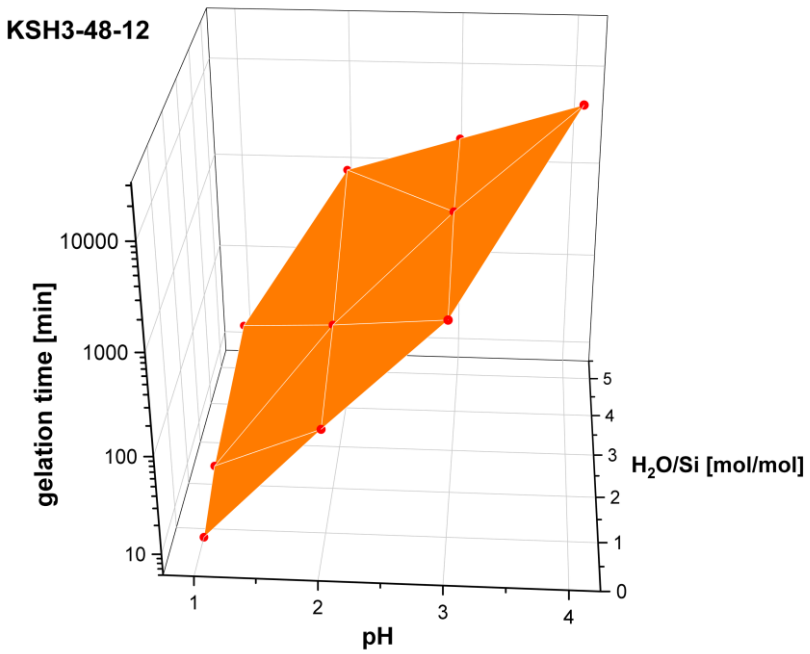

Figure 35: Combined dependence of the three studied parameters, namely gelation time, pH and H_2O/Si ratio for polymers KSH3-48 (12 wt.%).

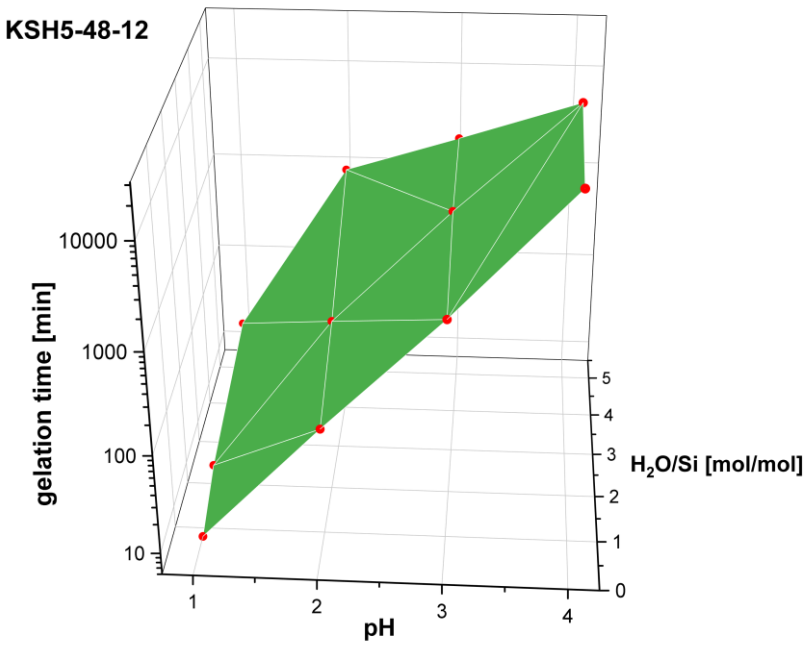

Figure 36: Combined dependence of the three studied parameters, namely gelation time, pH and H_2O/Si ratio for polymers KSH5-48 (12 wt.%).

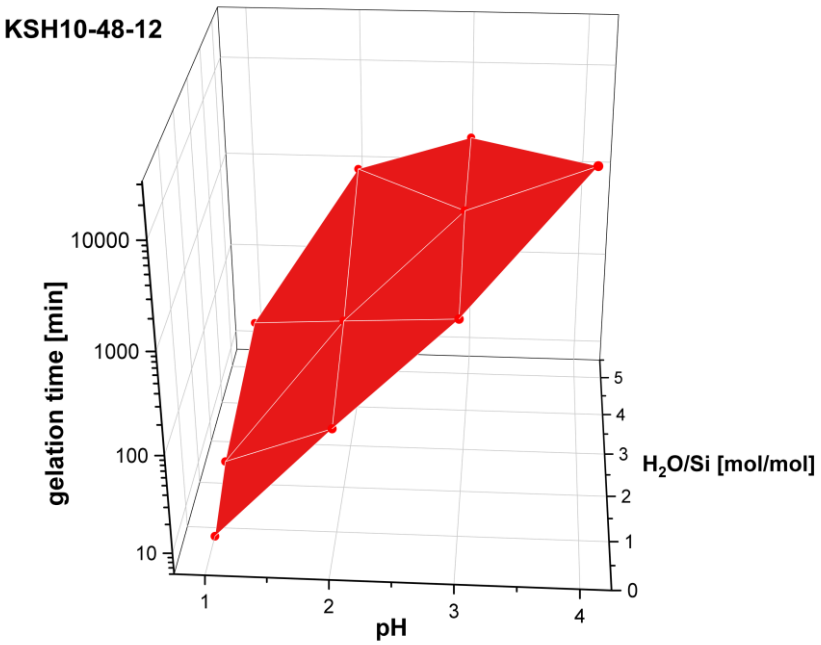

Figure 37: Combined dependence of the three studied parameters, namely gelation time, pH and H_2O/Si ratio for polymers KSH10-48 (12 wt.%).

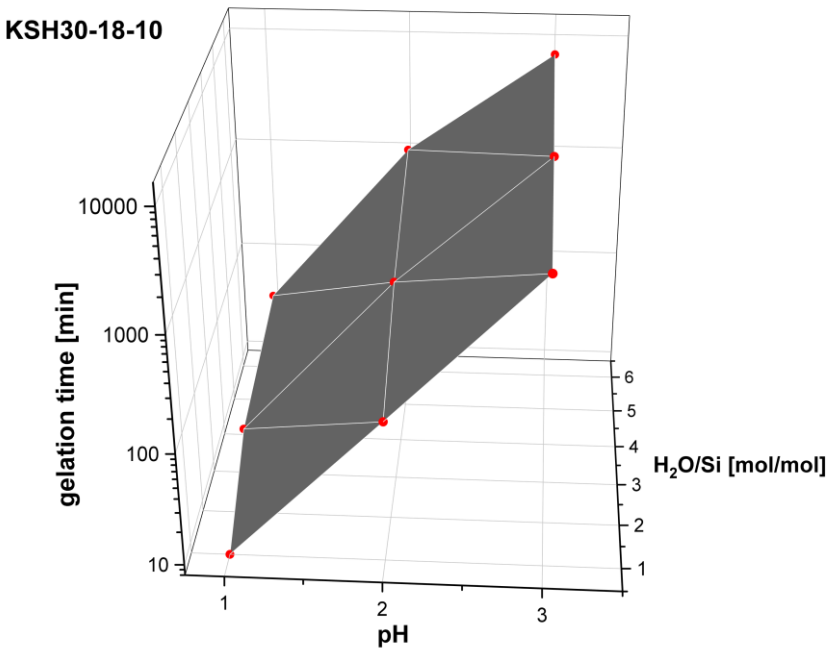

Figure 38: Combined dependence of the three studied parameters, namely gelation time, pH and H_2O/Si ratio for polymers KSH30-18 (10 wt.%).